The vertical BLR structure in nearby AGN

Wolfram Kollatschny, Göttingen

Austin, 2014

Bev and I, summer 96

Broad emission line profiles contain information on the kinematics and structure of the line emitt. regions

Line profiles can be parametrized by their FWHM, line dispersion σ, or their ratio FWHM/σ of the mean or rms line profiles.

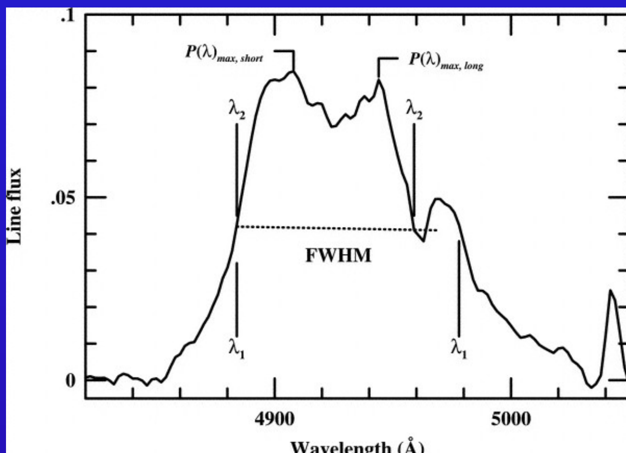

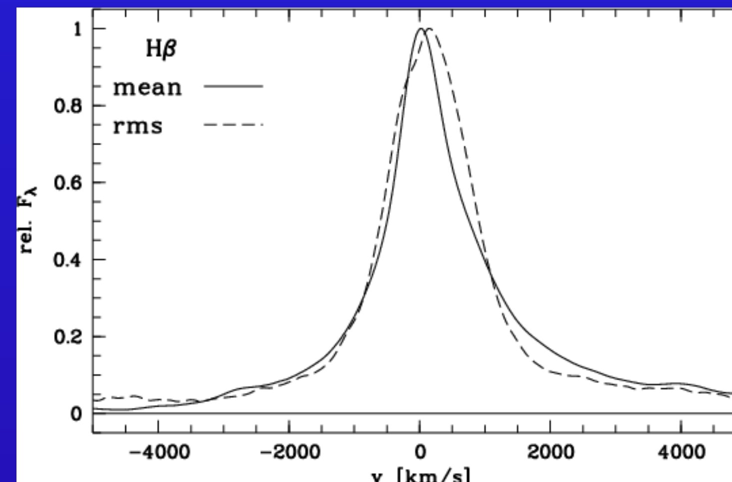

Line dispersion.—The first moment of the line profile is

$$\lambda_0 = \int \lambda P(\lambda) d\lambda \Big/ \int P(\lambda) d\lambda. \quad (4)$$

We use the second moment of the profile to define the variance or mean square dispersion

$$\sigma^2_{\rm line}(\lambda) = \langle \lambda^2 \rangle - \lambda_0^2 = \left[\int \lambda^2 P(\lambda) d\lambda \Big/ \int P(\lambda) d\lambda \right] - \lambda_0^2. \quad (5)$$

The square root of this equation is the line dispersion $\sigma_{\rm line}$ or rms width of the line.

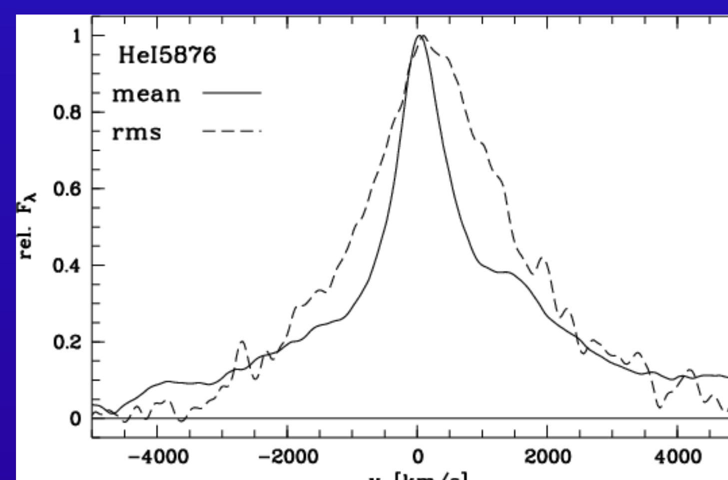

Peterson et al., 2004

Mrk110 Kollatschny, 2003

Line-width ratios FWHM/σ for different line profiles

Different motions lead to different emission line profiles.

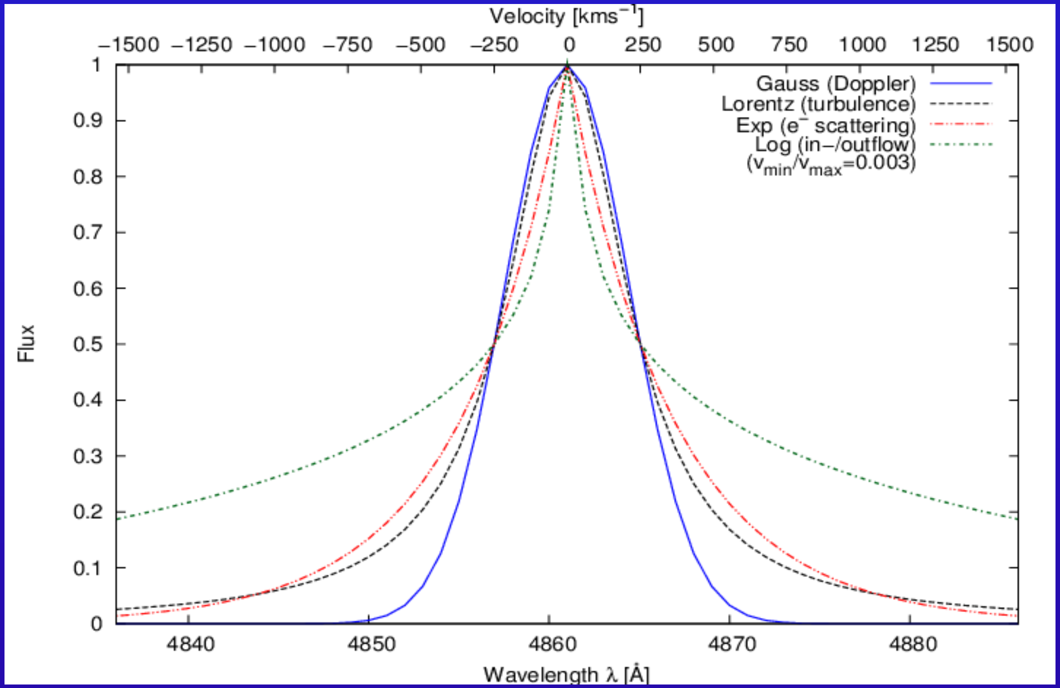

Relationship between FWHM and σ depends on the line profile:

	FWHM/σ
- rectangular fct.	3.46
- edge-on rotat. ring	2.83
- Gaussian profile	2.35
- exponent. profile	√2*ln2≈0.98
- logarithmic profile	→ 0.
- Lorentzian profile	→ 0.

Hβ line-width ratio FWHM/σ versus σ

FWHM/σ observations of a data set of 35 variable AGN (from Peterson et al., 2004)

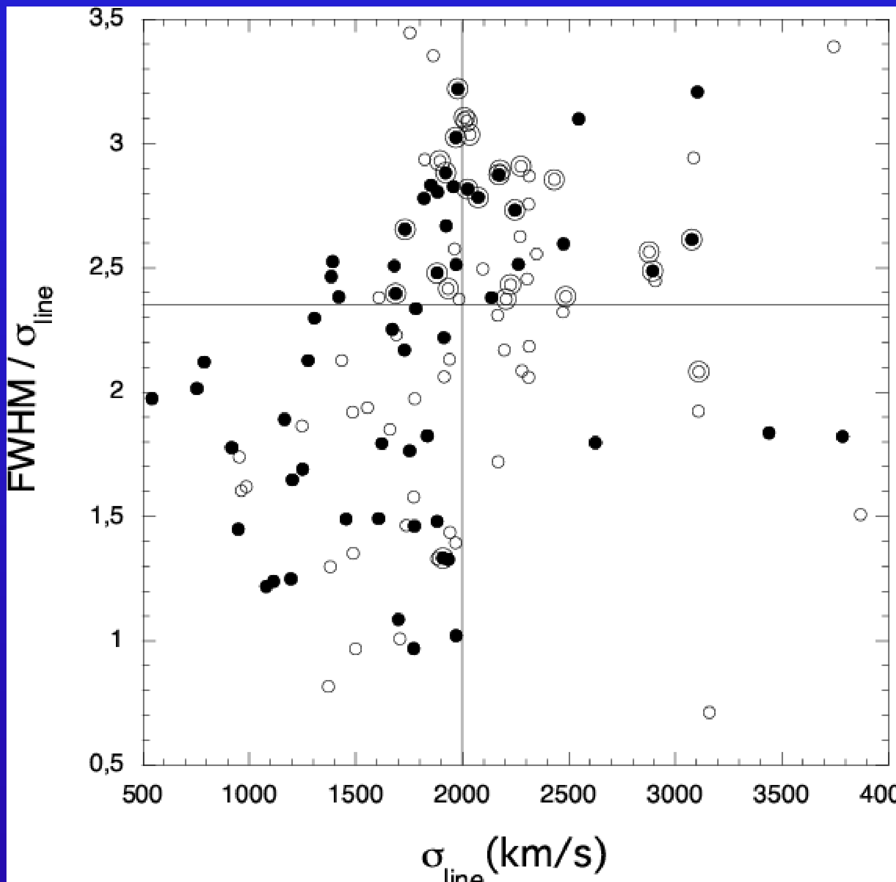

Collin et al., 2006

Relationship between FWHM and σ :

	FWHM/σ
- rectangular fct.	3.46
- edge-on rotat. ring	2.83
- triangular fct.	2.45
- Gaussian profile	2.35
- Lorentzian profile	→ 0.

Open and filled circles correspond to values based on mean and rms spectra.

The vertical line at σ = 2000 km/s approximates the division of Sulentic et al. (2000) into Populations A (left) and B (right).

The horizontal line at 2.35 divides the samples into Populations 1 (lower) and 2 (upper) (Collin et al., 2006).

Hβ line-width ratios: FWHM/σ vs. σ or vs. FWHM

Collin et al., 2006

Kollatschny & Zetzl, 2011, Nature 470

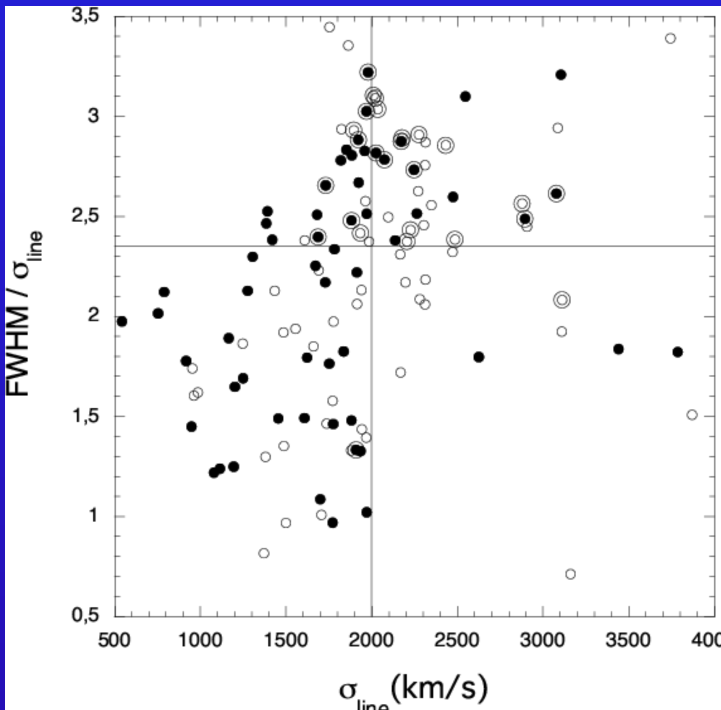

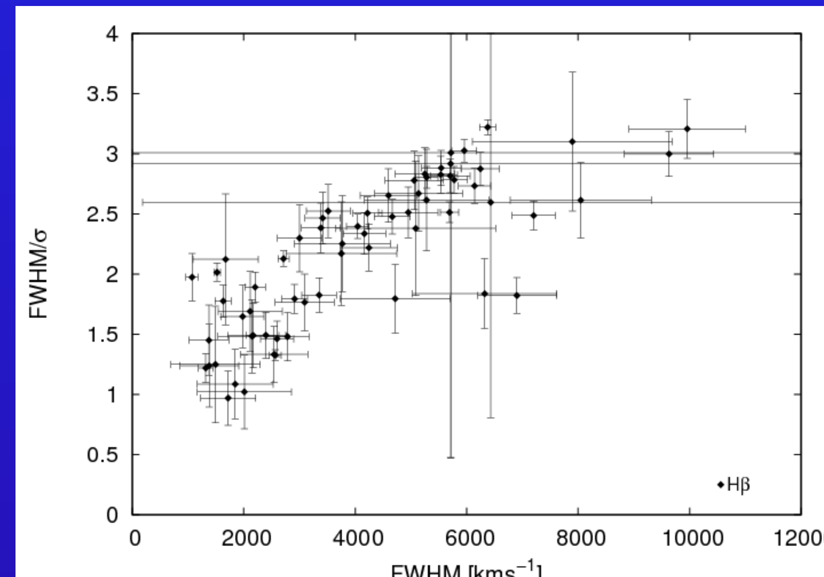

Hβ

The Hβ line-width ratio FWHM/σ versus σ (mean & rms profiles).

Table 1 | Line profile versus linewidth correlations

	r_p	r_s	r_k	P_p	P_s	P_k
Hβ FWHM/σ_{line} versus FWHM	0.792	0.823	0.649	6.4×10^{-15}	6.4×10^{-11}	3.5×10^{-14}
Hβ FWHM/σ_{line} versus σ_{line}	0.364	0.513	0.350	0.003	4.7×10^{-5}	4.4×10^{-5}
He II FWHM/σ_{line} versus FWHM	0.803	0.786	0.571	0.016	0.041	0.048
He II FWHM/σ_{line} versus σ_{line}	0.464	0.357	0.214	0.247	0.361	0.458
C IV FWHM/σ_{line} versus FWHM	0.821	0.821	0.619	0.023	0.049	0.051
C IV FWHM/σ_{line} versus σ_{line}	0.599	0.643	0.429	0.155	0.126	0.176

Given are the Pearson correlation coefficient r_p, the Spearman's rank-correlation coefficient r_s, as well as the Kendall correlation coefficient r_k for Hβ, He II $\lambda = 4{,}686$ Å and C IV $\lambda = 1{,}550$ Å linewidth ratios FWHM/σ_{line} versus FWHM as well as FWHM/σ_{line} versus σ_{line}. P_p, P_s and P_k are the associated percentage probabilities for random correlations[15,16]. The Pearson correlation coefficient tests a linear relation only, while the other correlation coefficients test for a general monotonic relation.

Kollatschny & Zetzl: The Hβ line-width ratio FWHM/σ versus FWHM (rms profiles)

HeII and CIV line-width ratios FWHM/σ versus FWHM

From Peterson (2004) data set:

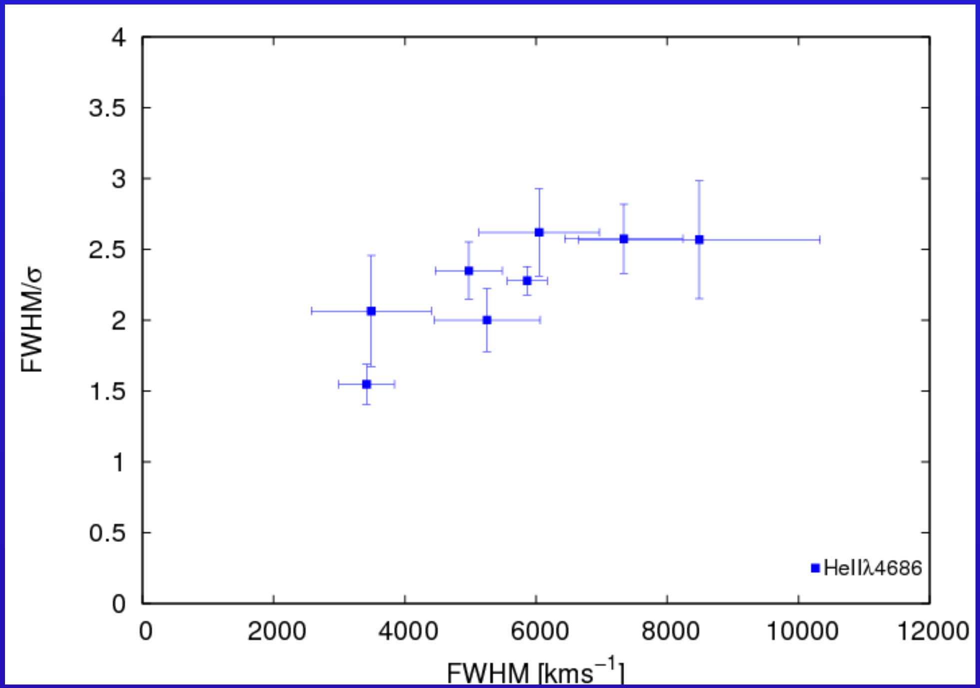

The HeIIλ4686 line-width ratio FWHM/σ versus FWHM (rms profiles).

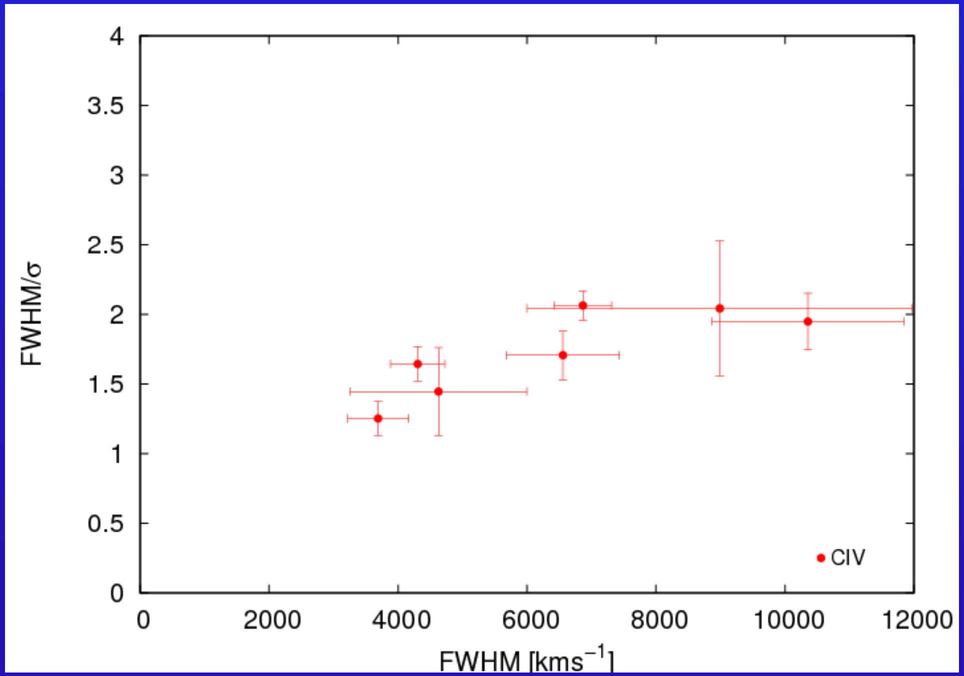

The CIVλ1549 line-width ratio FWHM/σ versus FWHM (rms profiles).

Kollatschny & Zetzl, 2011, Nature 470

Different emission lines show similar – however different – systematics in the line profile relations.

Line-width ratio studies

Observed Hβ, HeII and CIV line-width ratios FWHM/σ versus linewidth FWHM.

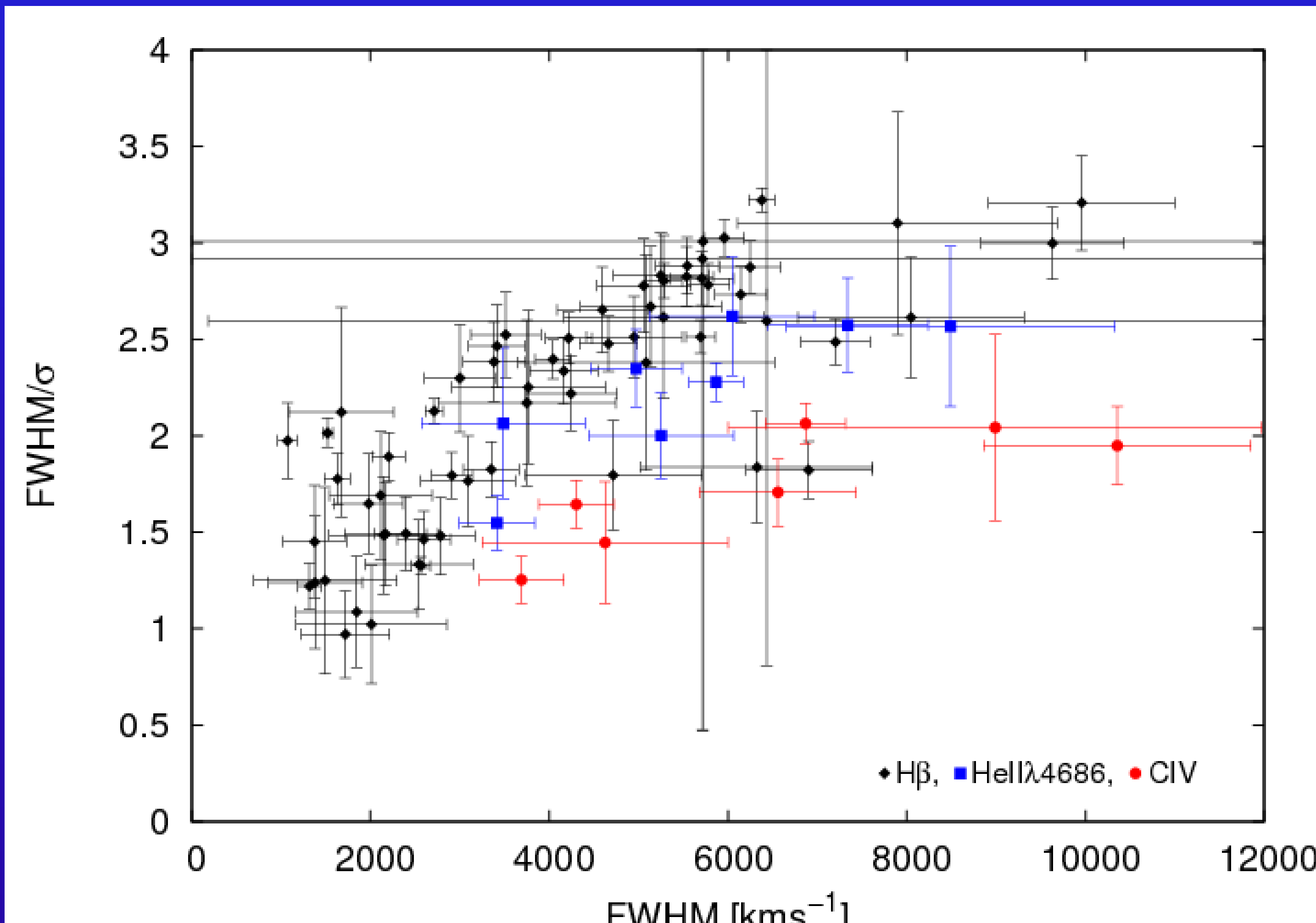

narrow prof.: steep

broad prof.: flat

Reproducing the observed trend(s) by simple convolution of few line profile types:

Modeling of observed line profile relations → FWHM, σ

Tests: *Theoretical line broadening of a Gaussian profile due to rotation and Doppler broadening of a Lorentzian profile .*

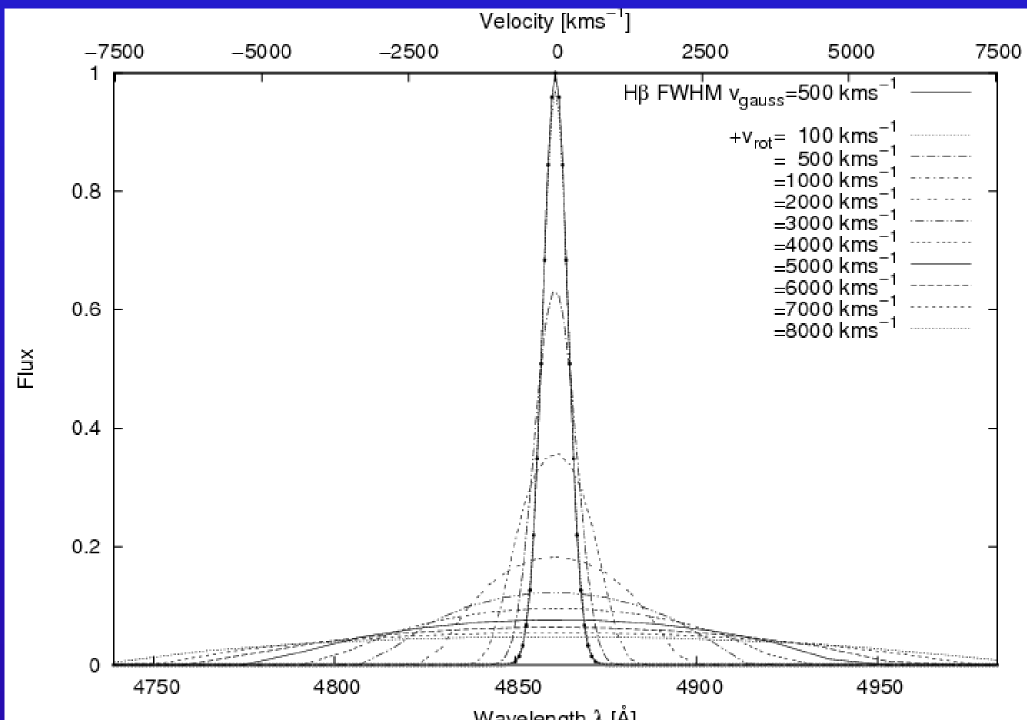

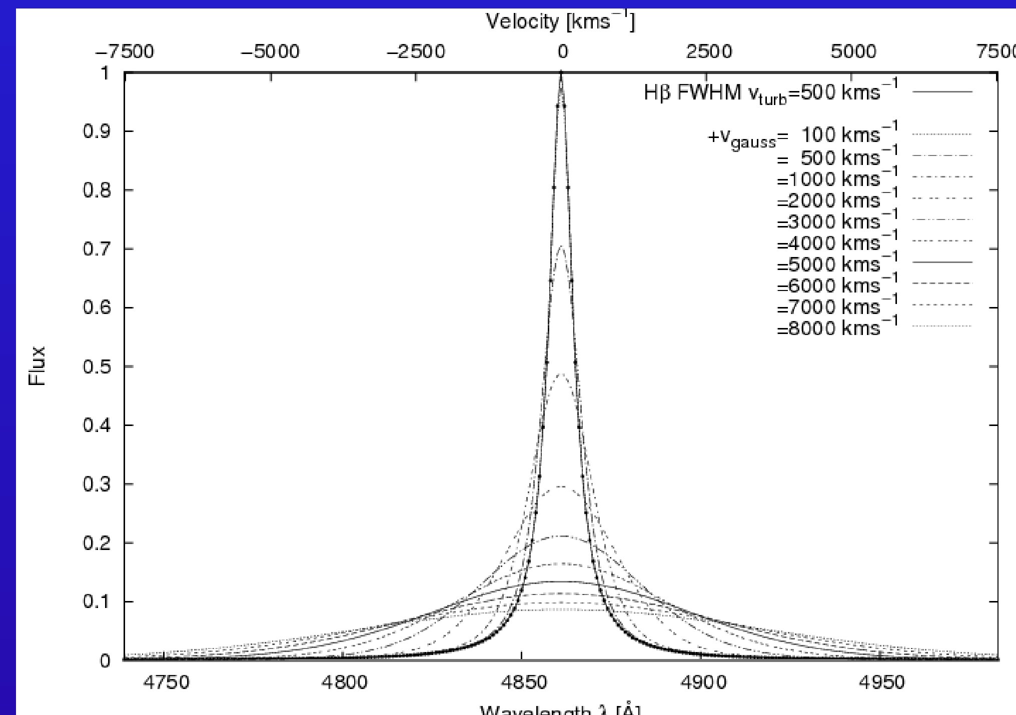

Rotational broadening of a Gaussian Hβ line profile ($v_{Doppler}$ = 500 km/s).

Doppler line broadening of Lorentzian Hβ profile (v_{turb} = 500 km/s).

Modeling of observed line profile relations

in simple way by multiple combinations of profiles.

Observed and theoretical Hβ line-width ratios FWHM/σ versus FWHM

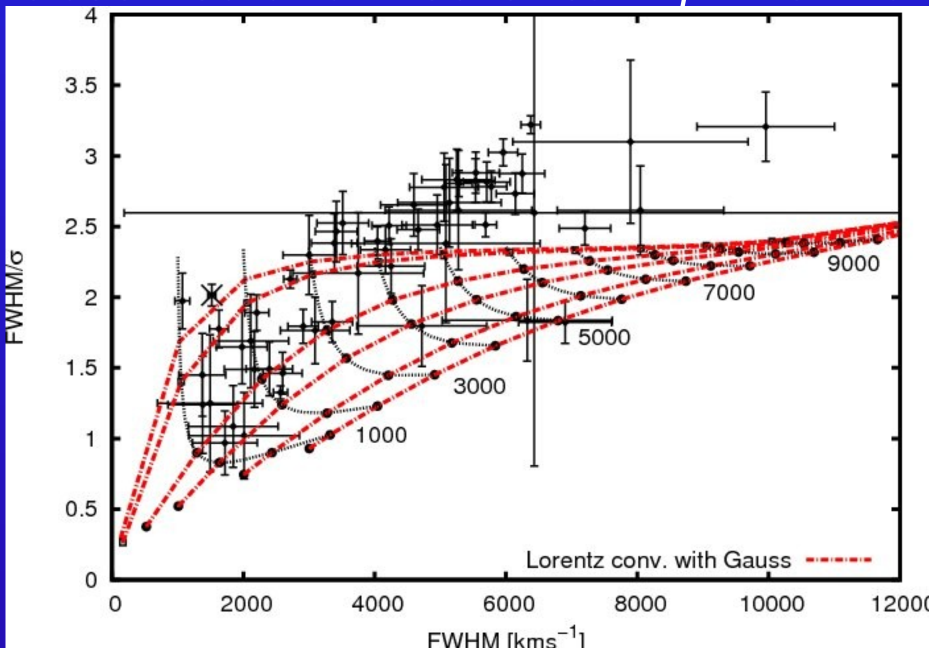

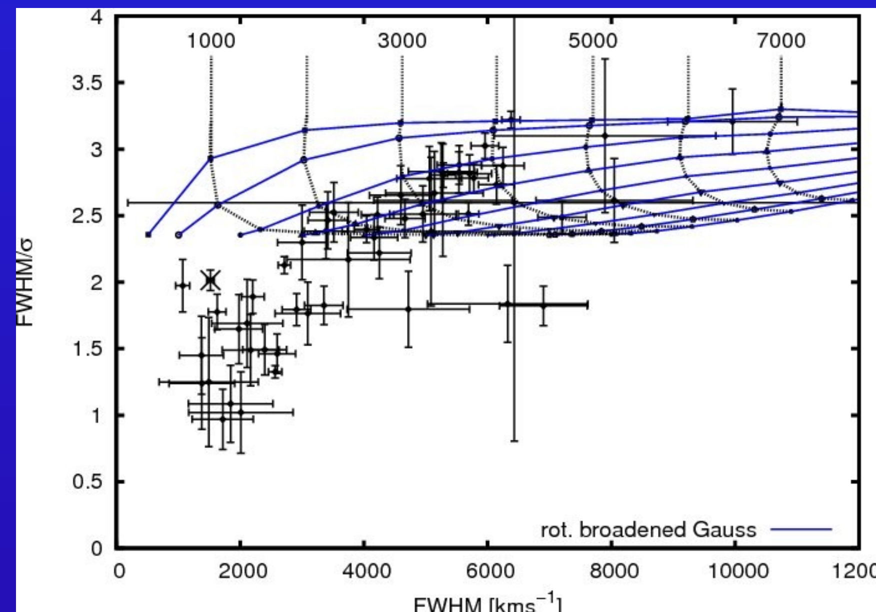

Lorentzian profiles convolved with Gaussian profiles.

The line widths of the Lorentzian profiles (FWHM) correspond to 50, 100, 500, 1000, 2000, 3000 km/s (from top to bottom). The widths of the Gaussian profiles correspond to 1000 to 9000 km/s (from left to right).

Rotational broadening of Gaussian profiles.

The line widths of the Gaussian profiles (FWHM) correspond to 500, 1000,..., 8000 km/s (from top to bottom). The associated rotational velocities range from 1000 to 7000 km/s (from left to right). FWHM/σ always larger than 2.35.

Kollatschny & Zetzl, 2011, Nature 470

Modeling the line broadening due to rotation

The rotational velocity b=Δλ/x is by definition the half width at zero intensity (HWZI) of an ellipsoidal profile (Unsoeld, 1955):

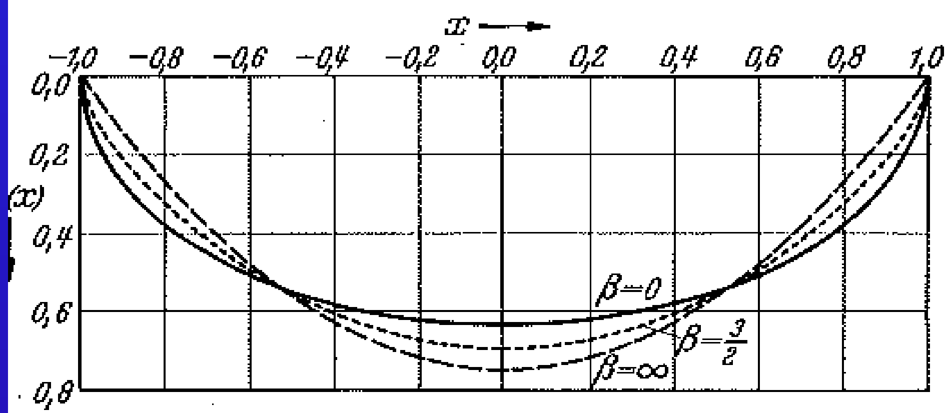

Abb. 168. „Rotationsprofil" $A(x) = \dfrac{\frac{2}{\pi}\sqrt{1-x^2} + \frac{\beta}{2}(1-x^2)}{1+\frac{2}{3}\cdot\beta}$ für verschiedene Werte des Randverdunkelungskoeffizienten β.

$$A(x) = \frac{2}{\pi}\sqrt{1-x^2}.$$

Line broadening formula:

$$S(y) = \int_{-\infty}^{+\infty} W(y-x)A(x)\,\mathrm{d}x$$

W: intrinsic line profile without rotational broadening, A: rotational profile
S: convolved profile

Modeling observed broad line profiles

Osterbrock *(78), Gaskell (09):*

Statistics of line widths imply that in addition to rotation there is a substantional velocity component perpendicular to the orbit plane: turbulence (Lorentzian profile).
The vertical component is also necessary for reconciling the structure of the BLR with its kinematics.

Modeling the observed line profile relations

Tests: *Theoretical line broadening of Lorentzian profiles due to rotation.*

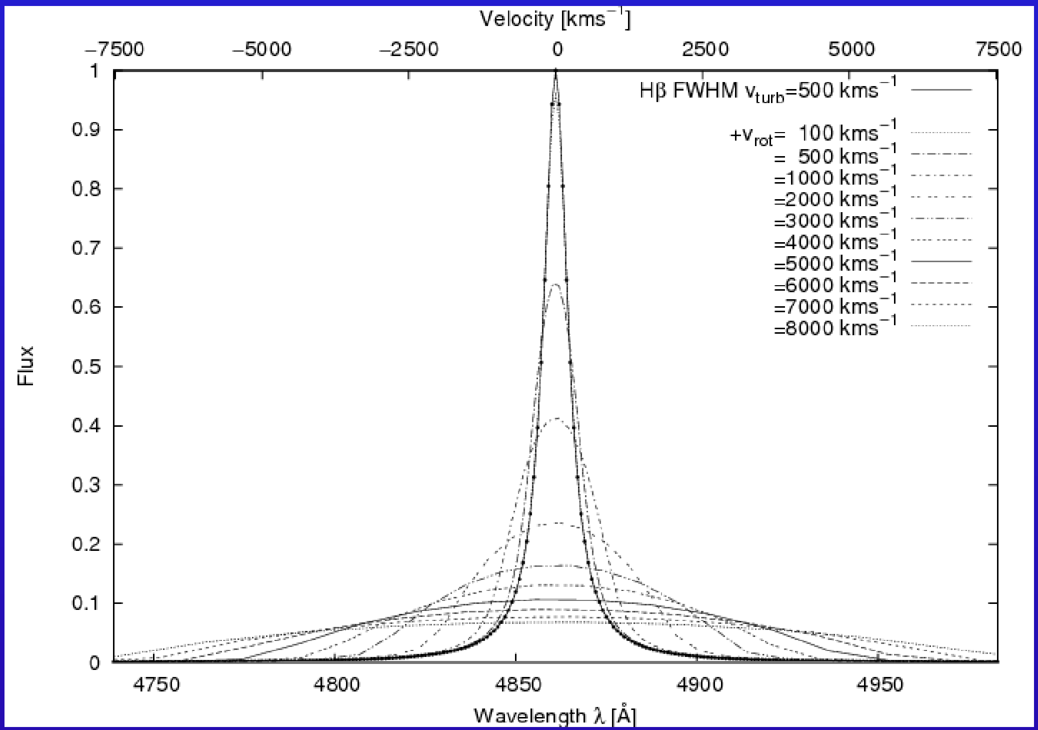

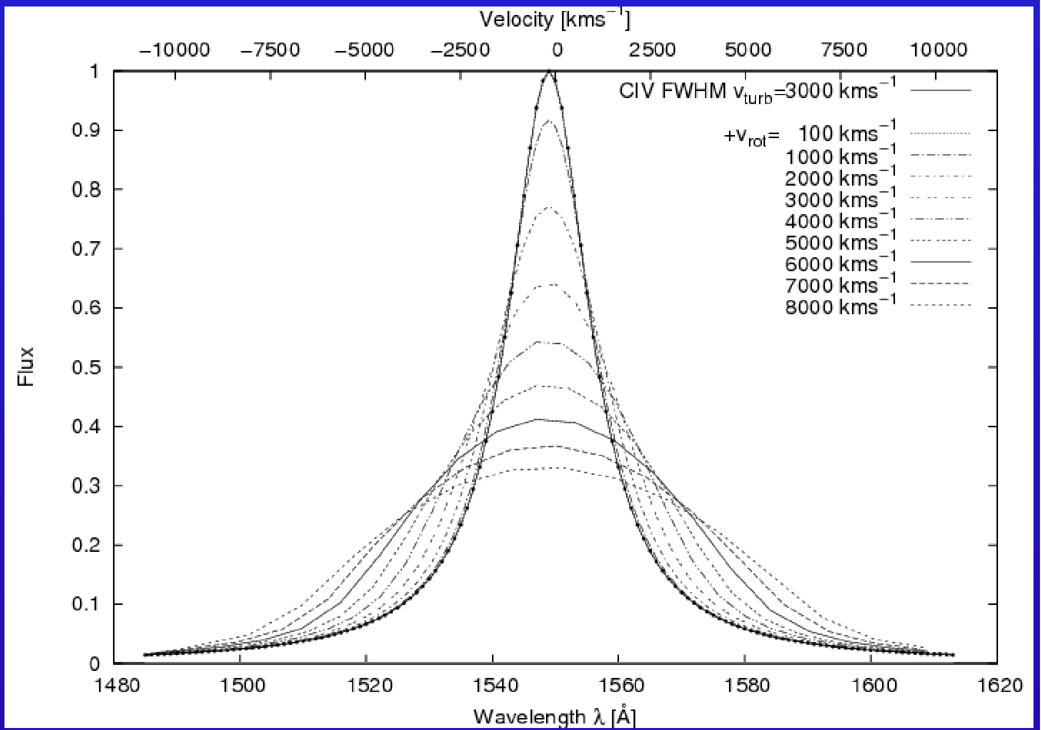

Rotational line broadening of Lorentzian Hβ profile (v_{turb} = 500 km/s).

Rotational line broadening of Lorentzian CIVλ1550 profile (v_{turb} = 3000 km/s).

Observed and modeled Hβ line widths ratios

General trends: FWHM/σ versus linewidth FWHM

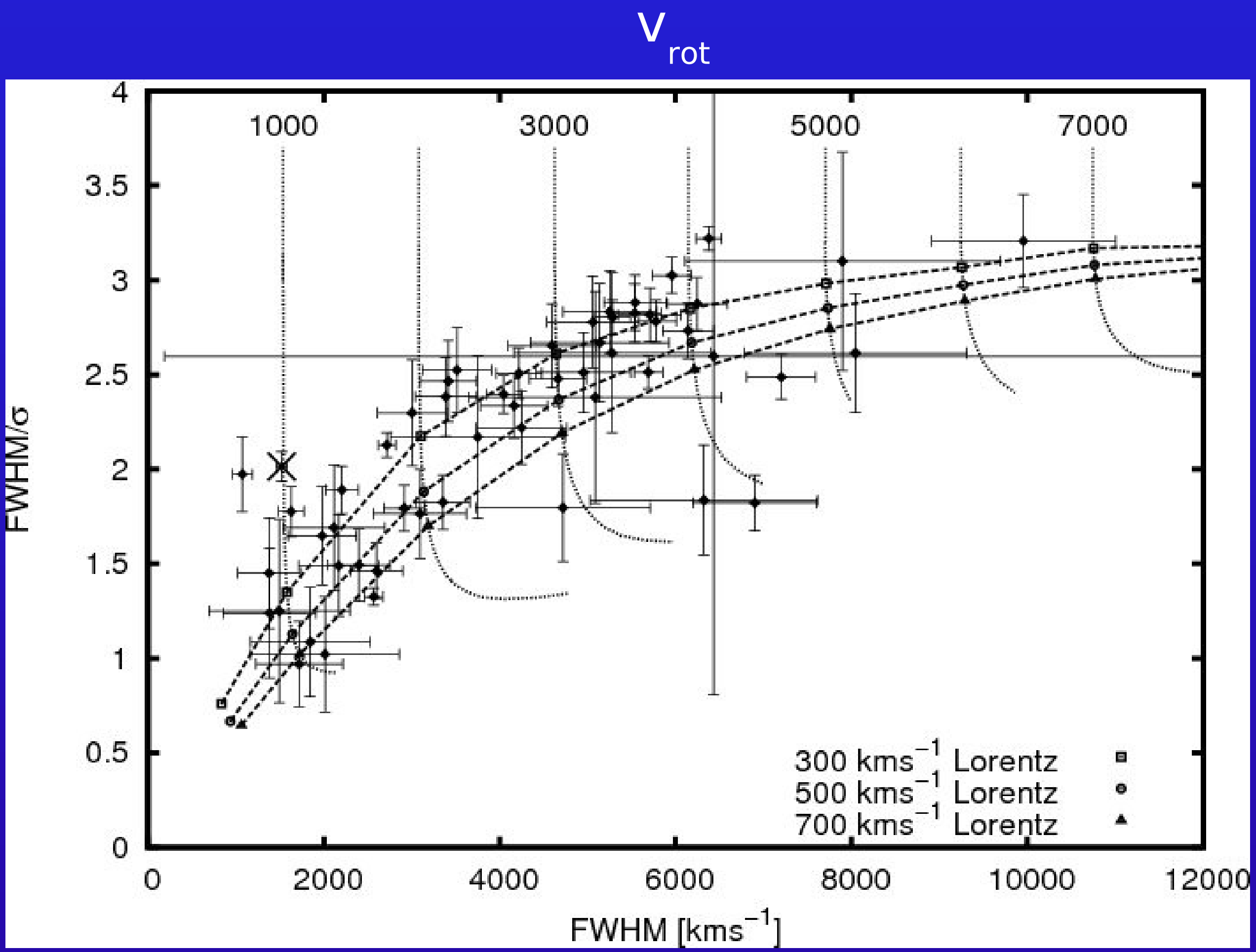

Dashed curves: rotational line broadened Lorentzian profiles (FWHM = 300, 500, 700 km/s). Rotational velocities range from 1,000 to 7,000 km/s.

Kollatschny & Zetzl, 2011, Nature 470

Observed and modeled HeII and CIV line widths ratios

FWHM/σ versus linewidth FWHM

HeIIλ4686

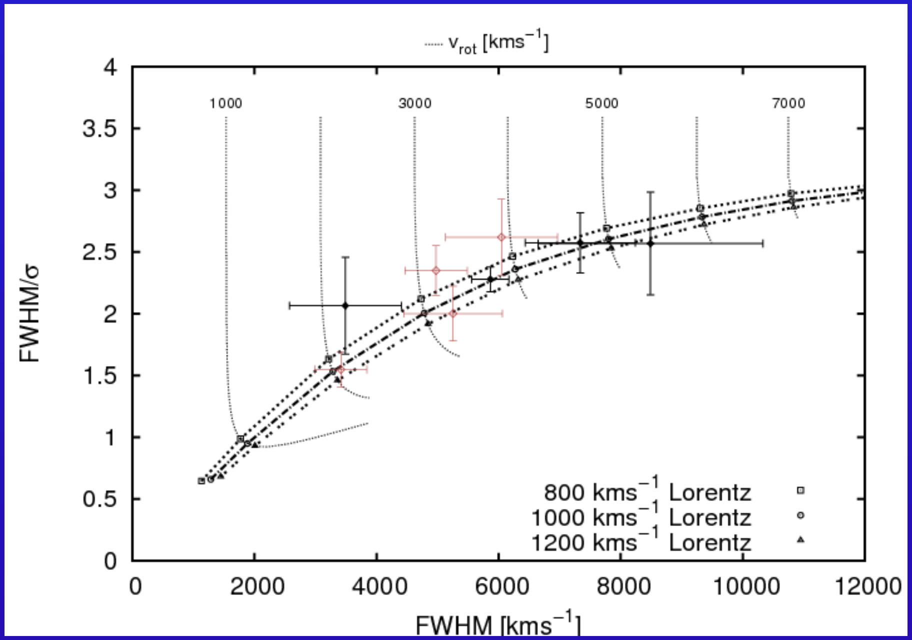

CIVλ1550

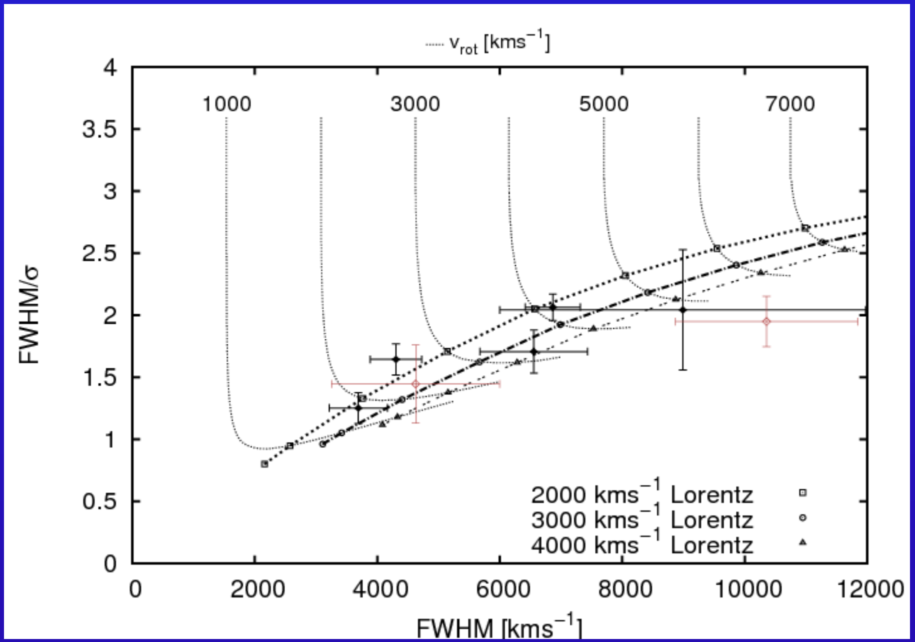

Dashed curves: theoretical linewidth ratios of rotational line broadened Lorentzian profiles (FWHM = 800; 1,000; 1,200 km/s). Rotational velocities range from 2,000 to 6,000 km/s.

Dashed curves: theoretical linewidth ratios of rotational line broadened Lorentzian profiles (FWHM = 2,000; 3,000; 4,000 km/s). Rotational velocities range from 1,000 to 6,000 km/s.

Line profile studies: BLR structure & kinematics

Observed and modeled Hβ, HeII and CIV line-width ratios FWHM/σ versus linewidth FWHM.

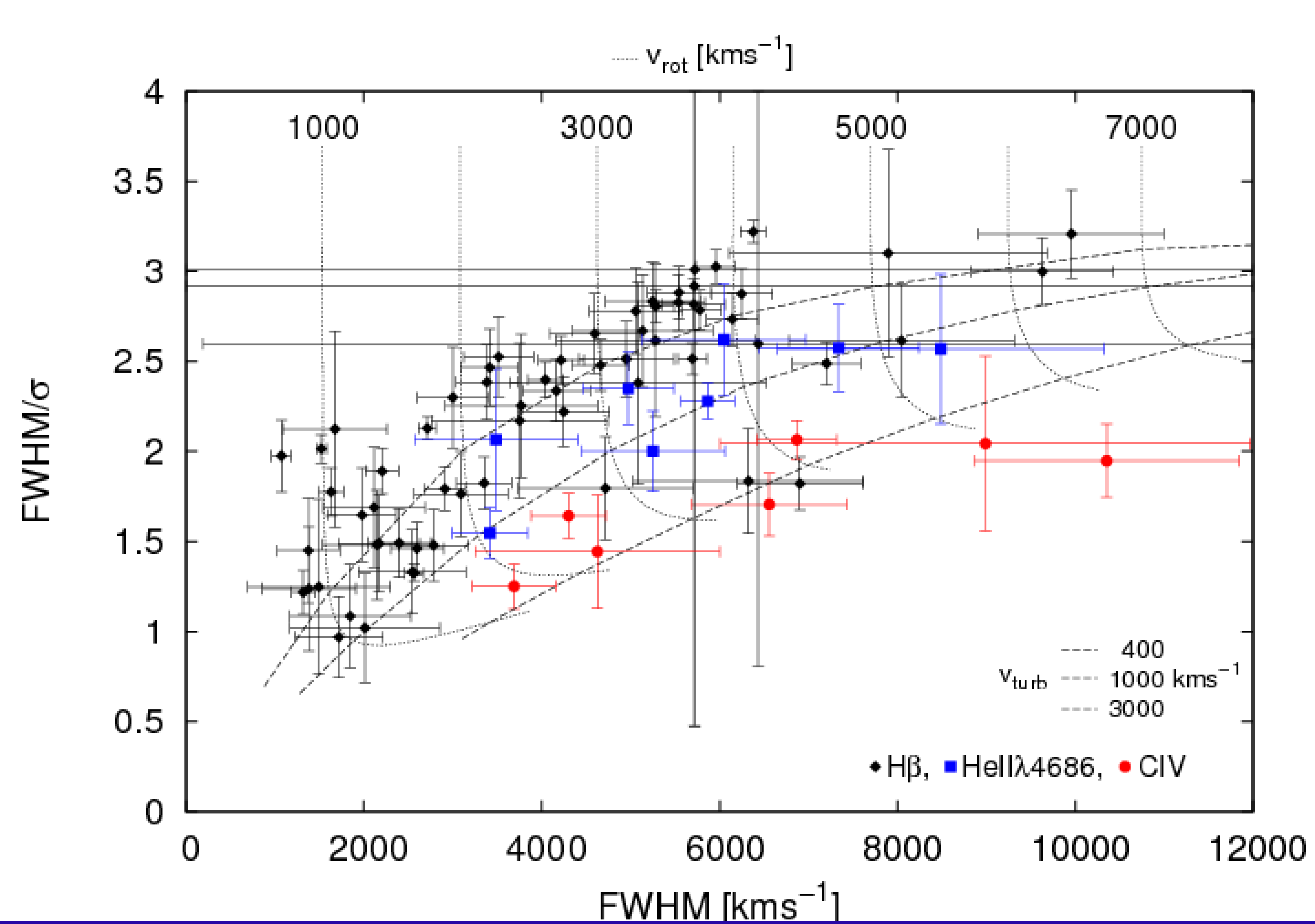

Kollatschny & Zetzl, 2011, 2013a

Line profile studies: BLR structure & kinematics

Characteristic turbulent velocities belong to individual emission lines in the BLR of all AGN:

- Hβ : 400 ± 200 km/s
- Hγ : 425 ± 125 km/s
- Hα : 700 ± 400 km/s
- HeIIλ4686 : 900 ± 250 km/s
- CIII]λ1909 : 1500 ± 700 km/s
- SiIV1400 : 2100 ± 900 km/s
- HeIIλ1640 : 2300 ± 1000 km/s
- CIVλ1549 : 2900 ± 1000 km/s
- Lyα+NVλ1240: 3800 ± 1400 km/s

Kollatschny & Zetzl 2013a

Observed and modeled Hβ line-width ratios FWHM/σ versus line-width FWHM

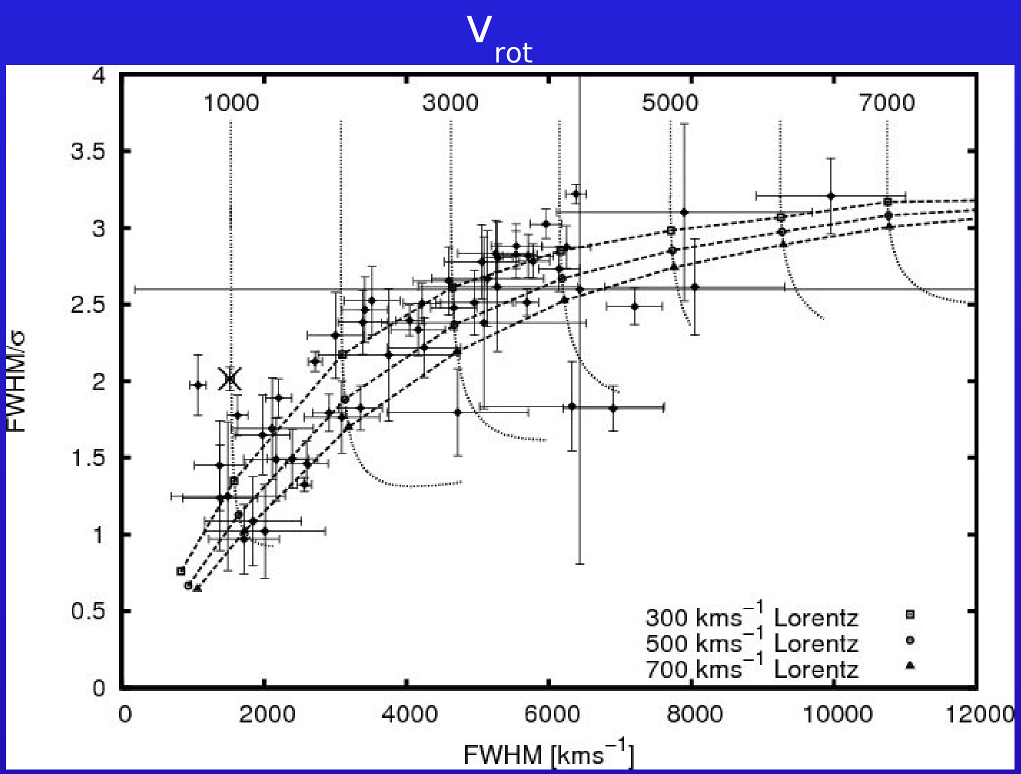

All AGN: Hβ turbulent velocity ~ 400 km/s

Rotation velocity differs in individual galaxies: 500 – 7,000 km/s

Deviations from general trend by e.g. orientation effects of line-em. accretion disk: *An inclined accretion disk leads to smaller line-widths owing to projection effects while the FWHM/σ remains constant (e.g. Mrk110 marked by a cross (i ~ 21°)).*

Further deviations by e.g. additional inflow/outflow components, obscuration,....

Correction factor for black hole masses

v_{rot}

$$M = \frac{f V_{\mathrm{FWHM}}^2 c\tau}{G}$$

Hβ

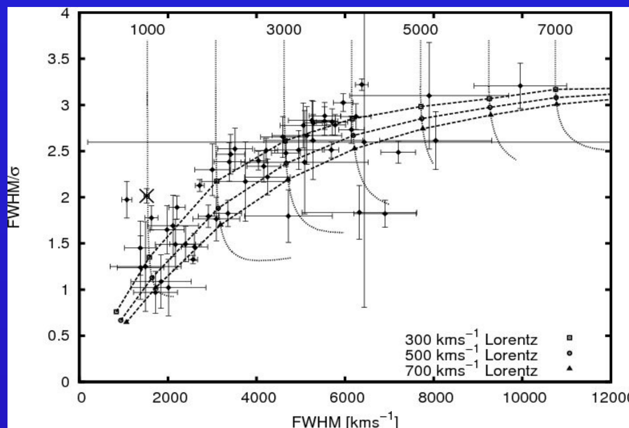

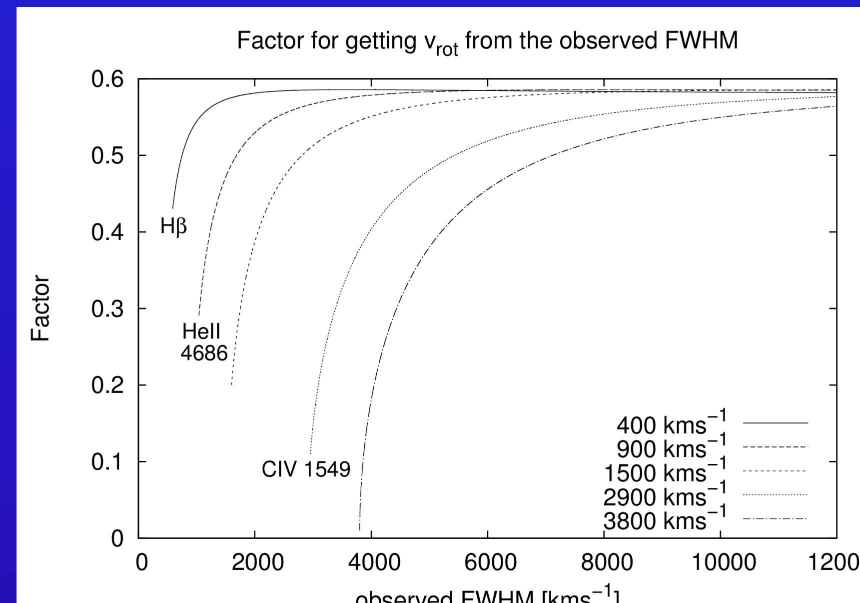

CIVλ1549

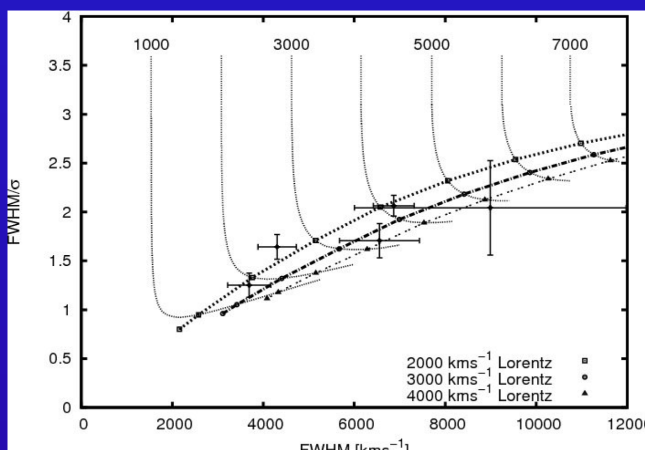

FWHM-correction factor for different em. lines (e.g. Hβ, CIVλ1549) for deriving the BH mass

Kollatschny & Zetzl, 2013a

- *narrow CIVλ1549 lines are rare (~2%) compared with narrow Hβ (~20%)* *(Baskin & Laor, 2005)*
- *different mass scaling relations are needed for the CIVλ1549 and Hβ line* *(Vestergaard .., 2006)*
- *the use of the CIVλ1549 line gives considerably different BH masses compared to Hβ* *(Netzer et al., 2007)*

Line profile studies: BLR structure & kinematics

From accretion disk theory (e.g. Pringle, 1981):

$$H(\text{eight}) / R(\text{adius}) = 1/\alpha \; * v_{turb} / v_{rot}$$

α = (const.) viscosity parameter

→ fast rotating broad line AGN: *geometrically thin accretion disk*

→ slow rotating narrow line AGN: *geometrically thick accretion disk*

Kollatschny & Zetzl, 2011, 2013a

Observed and modeled line-width ratios in NGC 5548

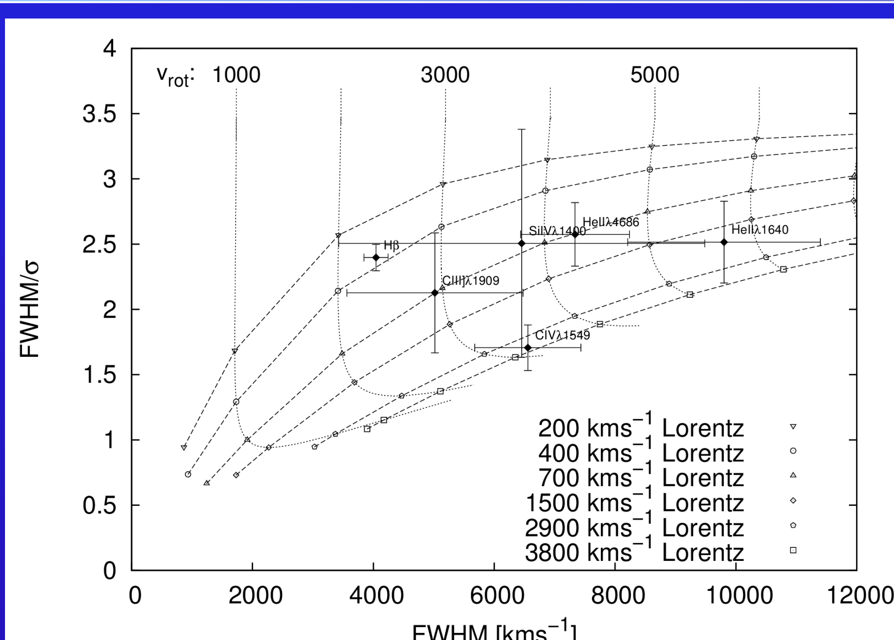

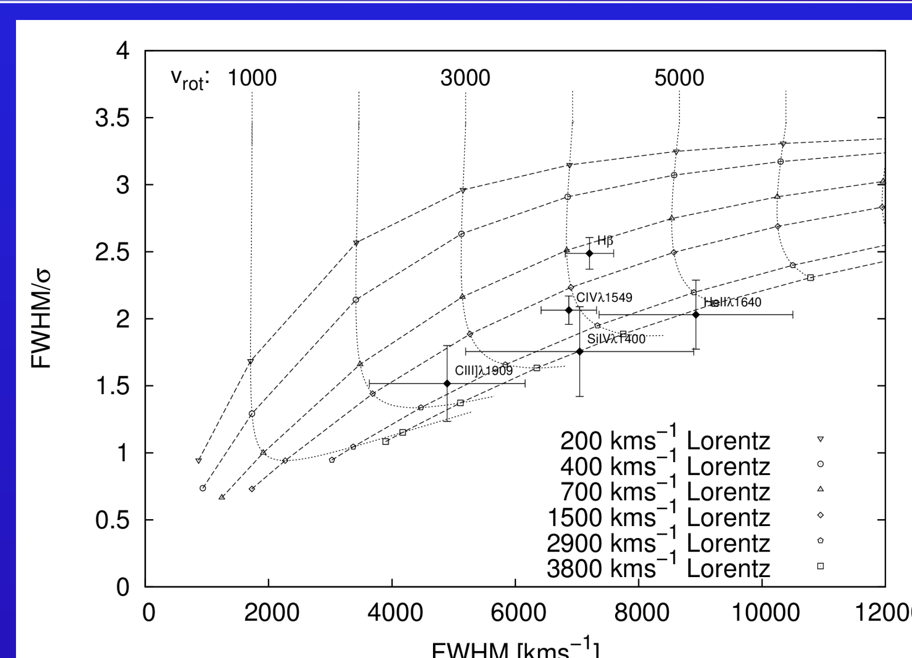

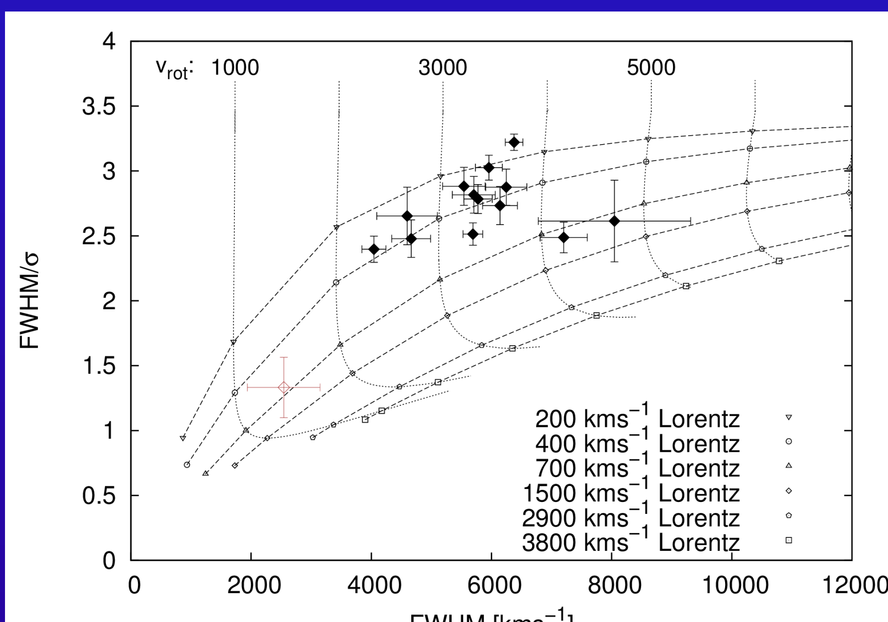

Observed and modeled line-width ratios FWHM/σ versus line-width FWHM for the periods 1988/89, 1992/93, and Hβ (1988-2001). Data from Peterson et al. (2004).

The dashed curves represent theoretical line width ratios based on rotational line broadened Lorentzian profiles (FWHM = 200 – 3800 km/s). The rotational velocities go from 1000 to 6000 km/s (curved dotted lines from left to right).

Kollatschny & Zetzl, 2013b

BLR structure in NGC 5548

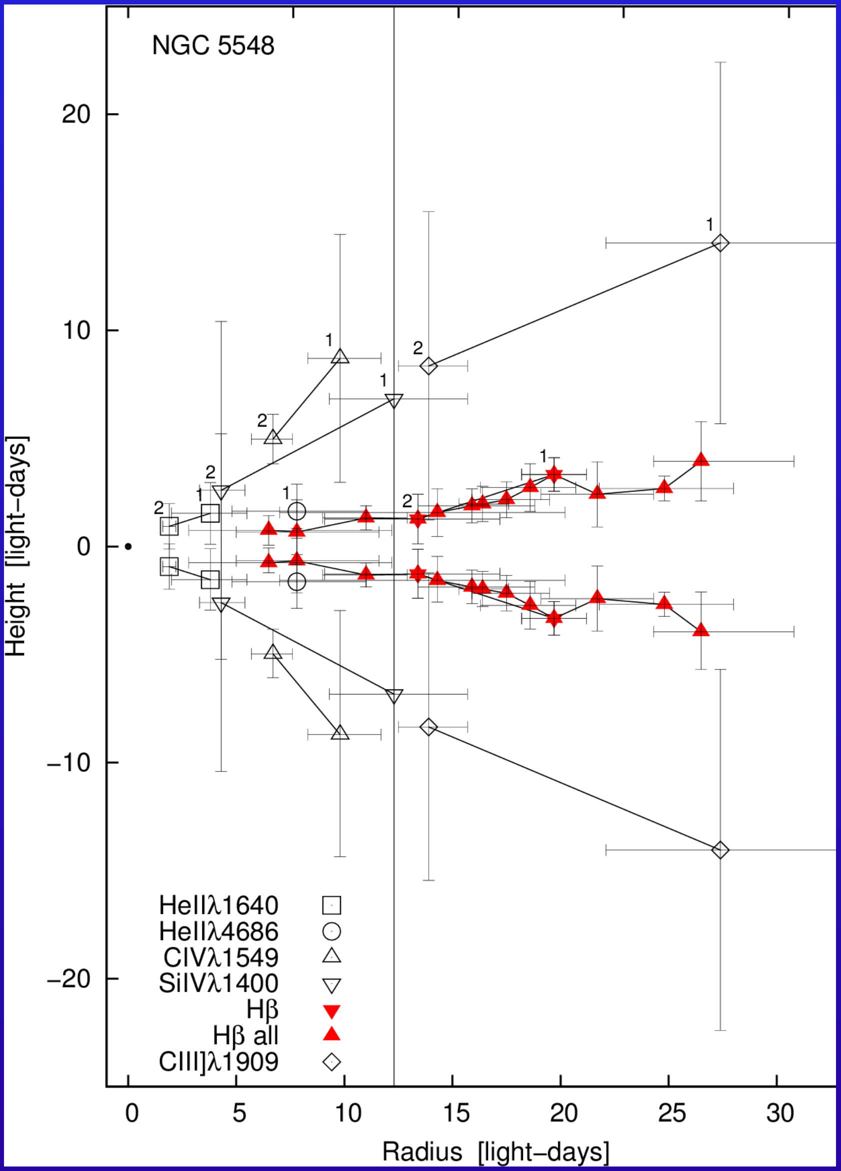

As we know v(turb) and v(rot) from modeling as well as the distances of the line emitting regions from the center (from reverberation mapping) we can estimate the heights of the line-emitting regions above the midplane. Hβ for 13 epochs, other lines for two/one epochs (connected by lines). Based on mean turbulent velocities.

The dot at radius zero gives the size of a Schwarzschild black hole (M=6.7x10^7Msolar) multiplied by a factor of twenty.

Kollatschny & Zetzl, 2013b

BLR structure in NGC 5548

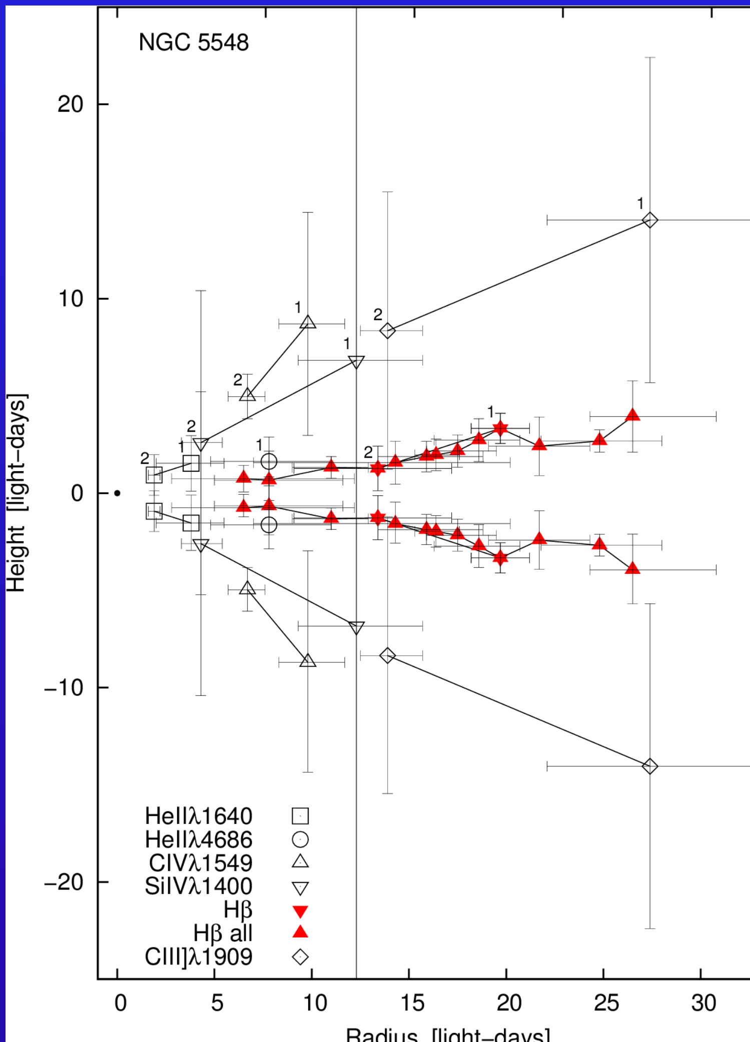

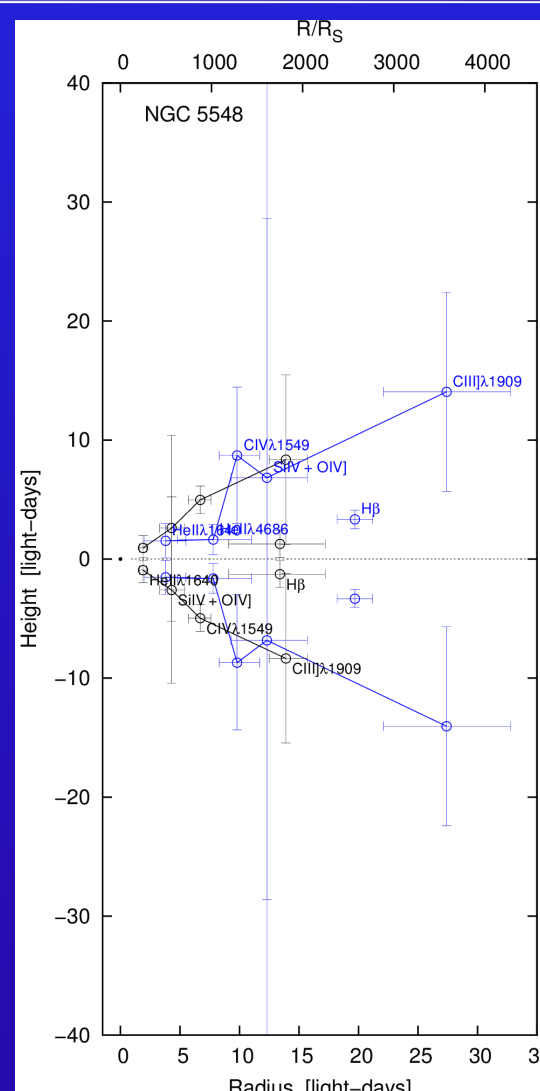

Hβ : 13 epochs; other highly ionized emission lines for two/one epochs (connected by lines).

Two epochs: 1988/89 (blue) and 1993 (black). Hβ kept separately; all other highly ionized emission lines connected by a solid line.

Kollatschny & Zetzl, 2013c

Observed and modeled line-width ratios in three AGN

NGC7469

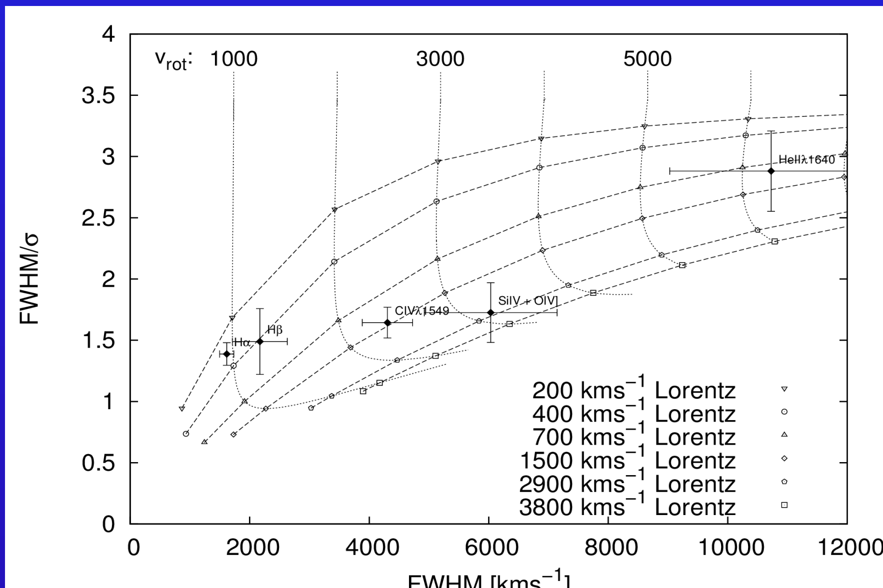

3C390.3

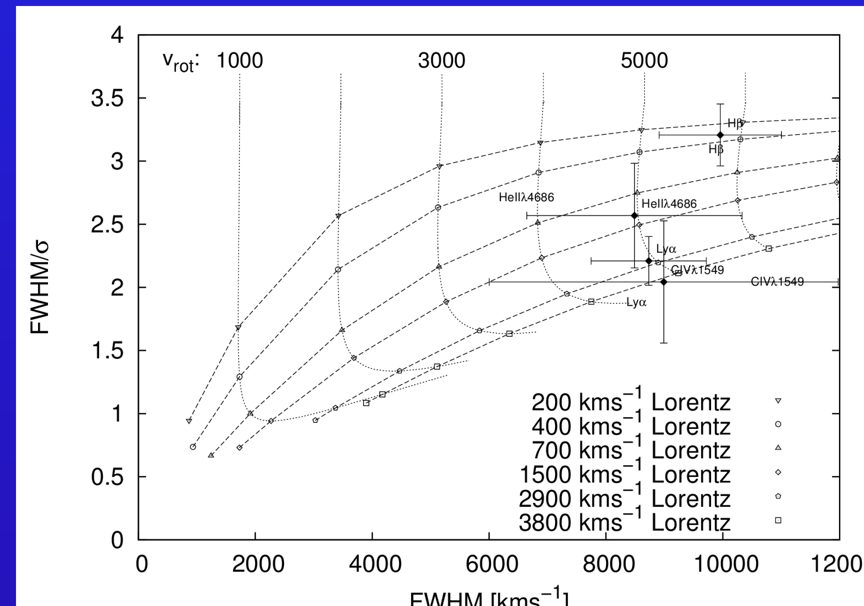

NGC3783

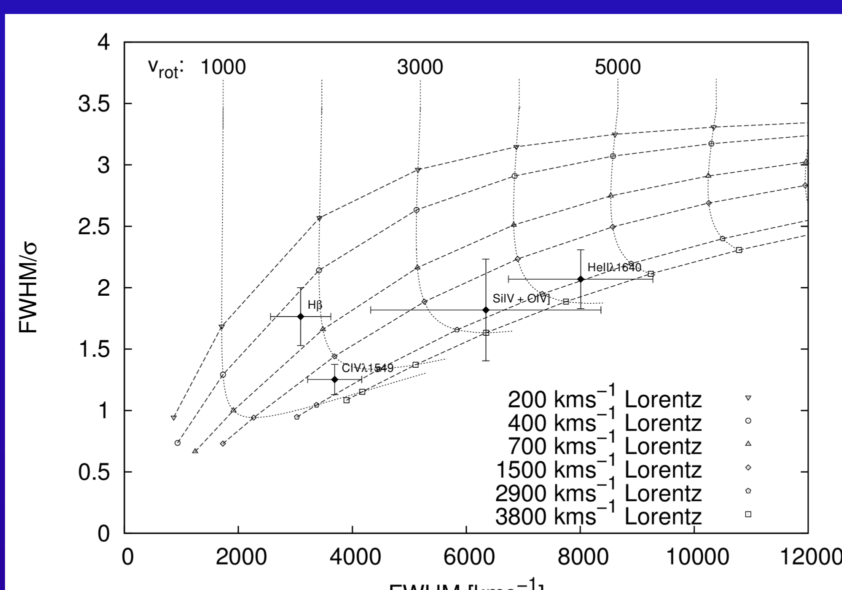

Observed and modeled line-width ratios FWHM/σ versus line-width FWHM for NGC7469, NGC3783, 3C390.3. Data from Peterson et al. (2004). At least four emission lines per galaxy.

Kollatschny & Zetzl, 2013c

BLR structures in NGC7469, NGC3783, 3C390.3

NGC7469

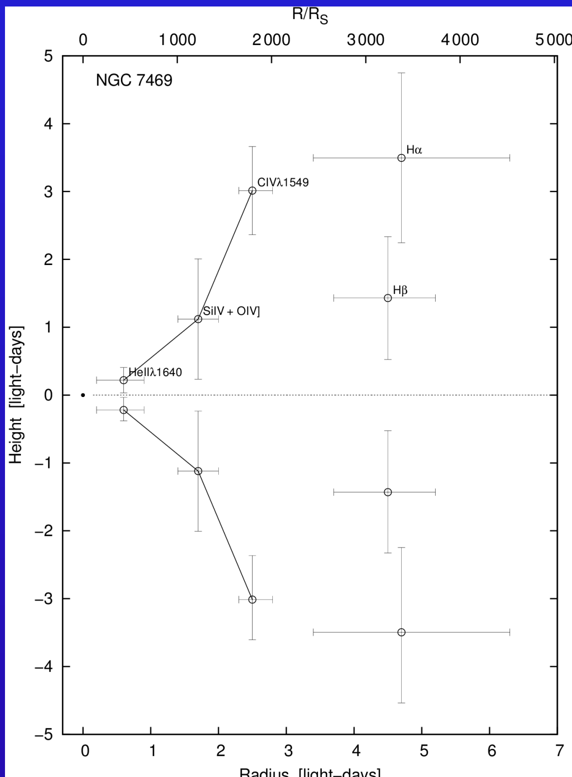

NGC3783

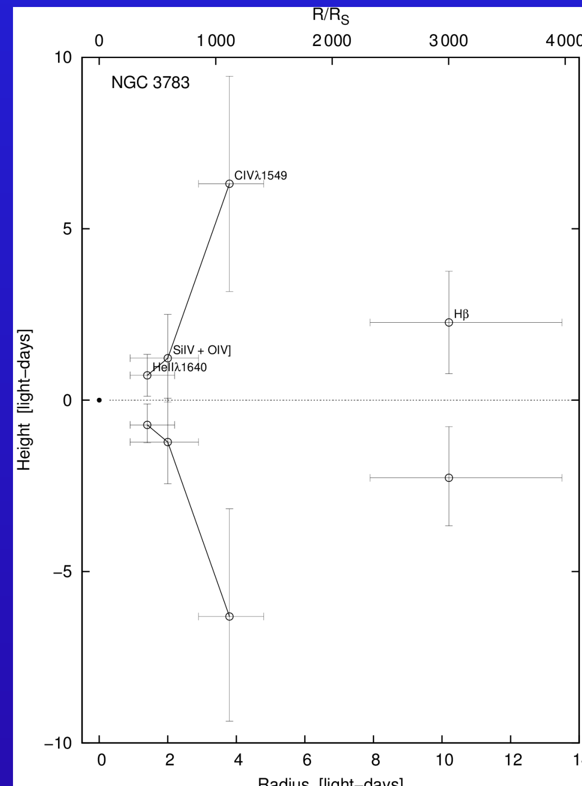

3C390.3

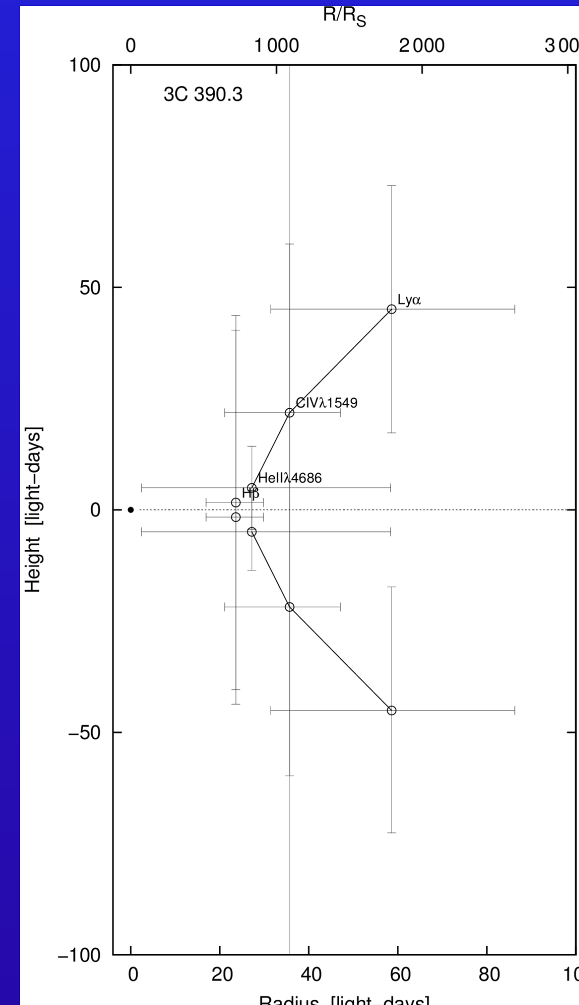

Highly ionized emission lines connected by a solid line. Balmer lines kept separately. Based on mean v(turb). The dot at radius zero gives the sizes of the individual Schwarzschild radii multiplied by a factor of twenty.

Kollatschny & Zetzl, 2013c

Observed + modeled line width ratios; BLR structure in 3C120

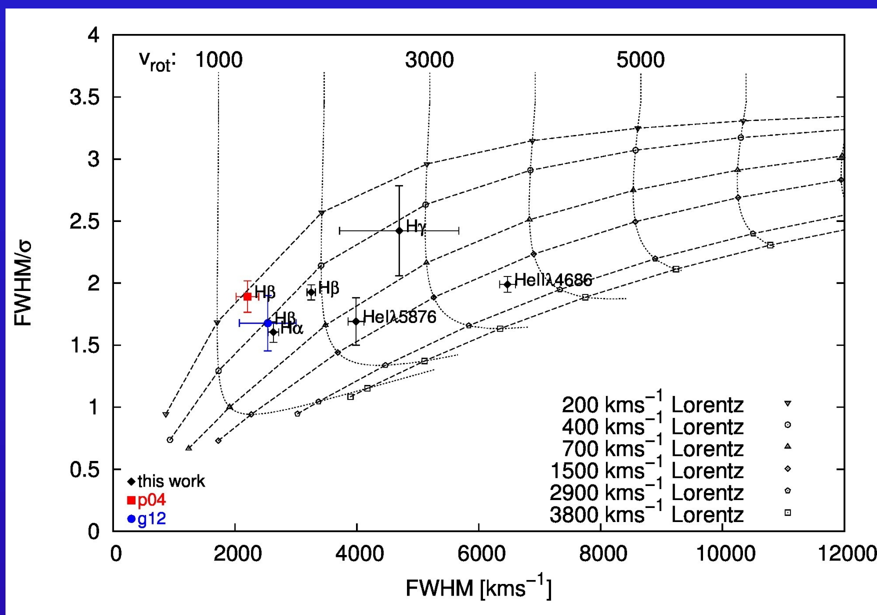

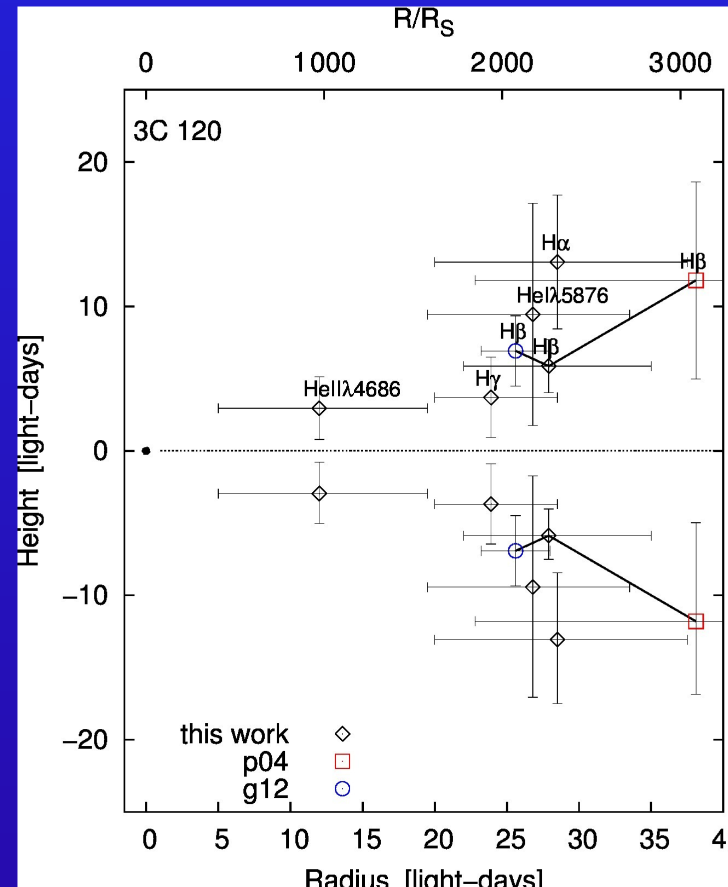

Hß observations from 3 variability campaigns (Peterson et al. 2004, Grier et al. 2012, Kollatschny et al. 2014).

Kollatschny & Zetzl, 2014

Comparison of BLR structures in AGN

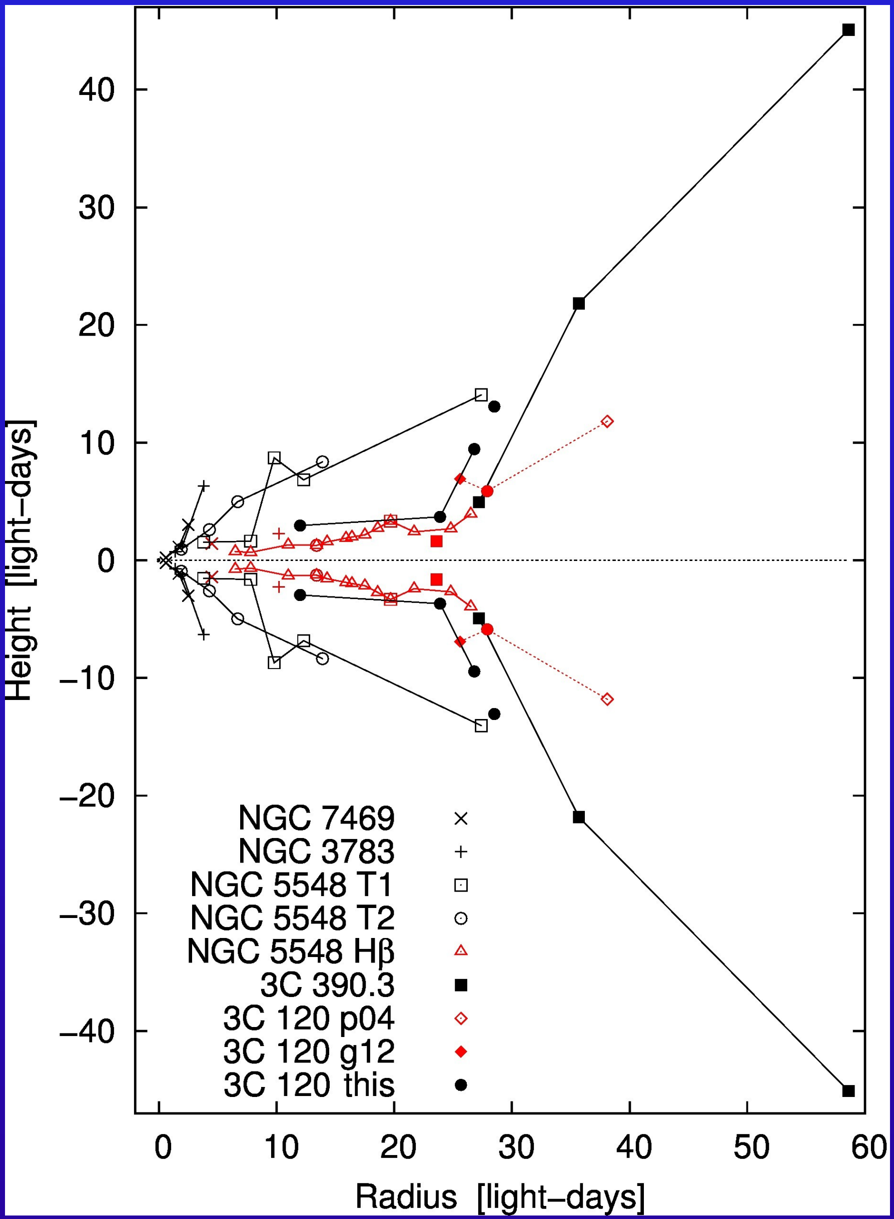

Comparison of the broad line region structures in NGC7469, NGC3783, NGC5548 (two epochs), 3C390.3 and 3C120 as a function of distance to the center as well as height above the midplane.

All the highly ionized emission lines of the individual galaxies are connected by a solid line.

Hβ emitting line regions are drawn in red. The Hβ emitting line regions in NGC5548 (13 epochs) are connected by a red solid line.

No simple scaling of one BLR structure only.

Kollatschny & Zetzl, 2013c, 2014

Hβ: Size-luminosity and FWHM-luminosity relation for AGN

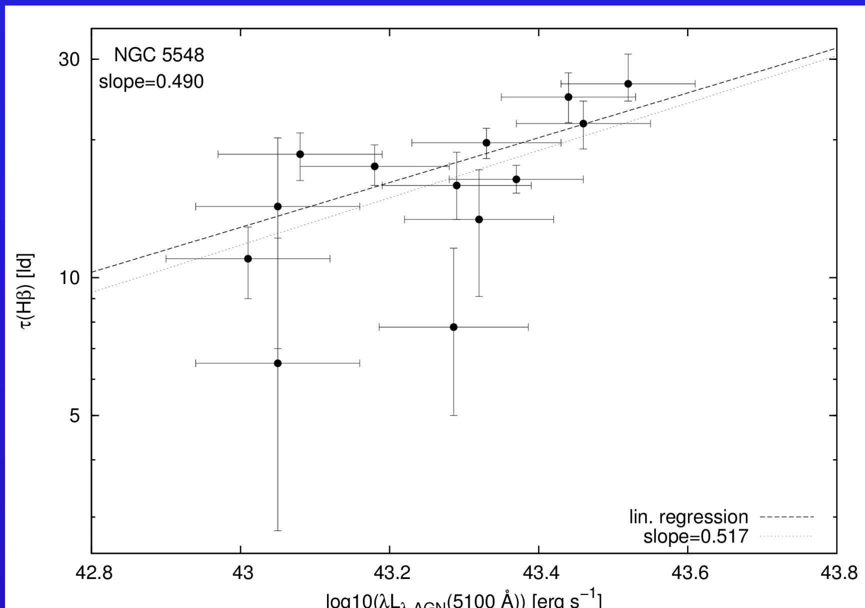

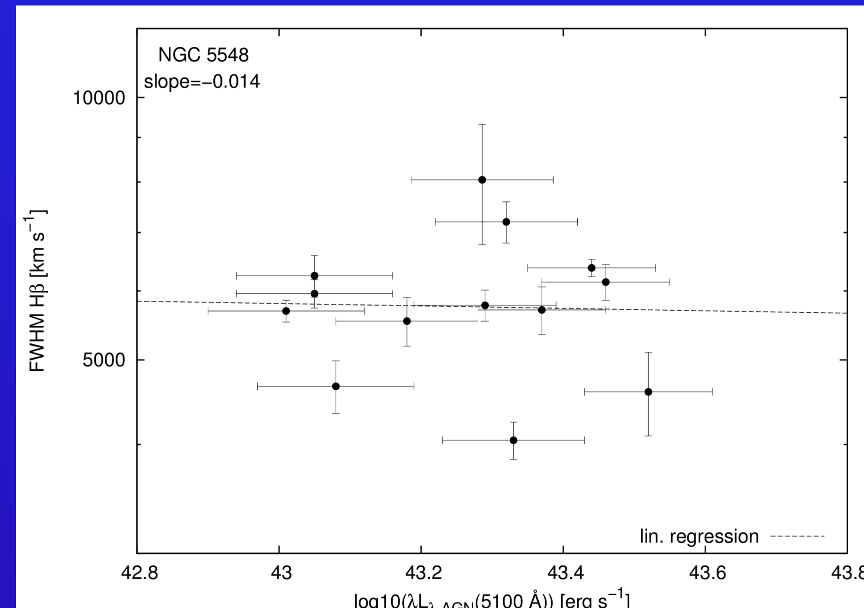

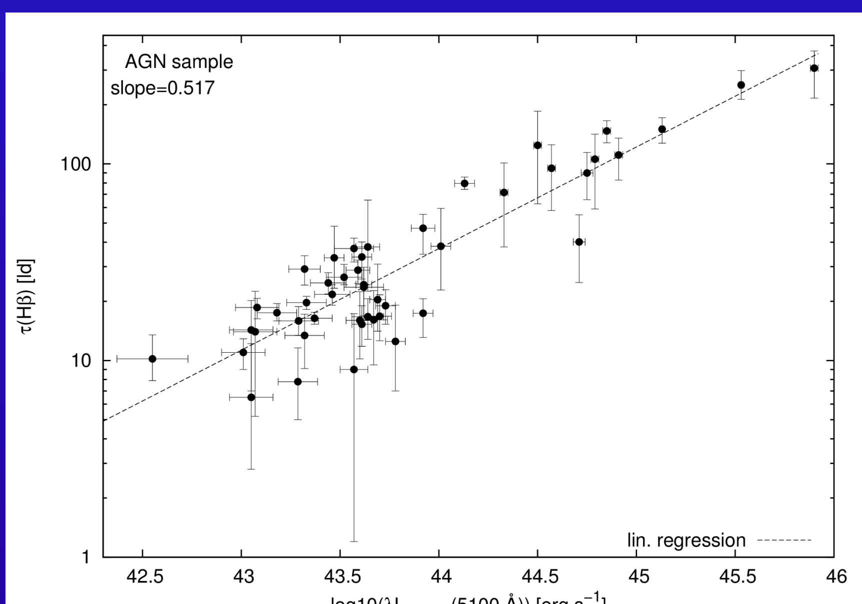

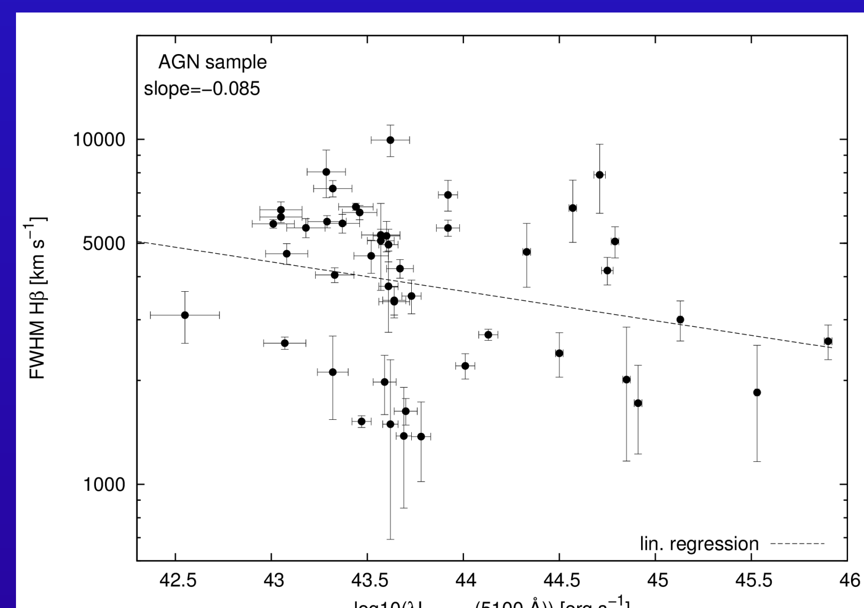

Peterson et al., 2004, AGN sample
corrected for host-galaxy contribution, Bentz et al., 2013

Kollatschny & Zetzl, 2013c

Hβ: Size-luminosity and FWHM-luminosity relation for AGN

Table 3. Correlation coefficients r (Pearson, Spearman, and Kendall) and probabilities P for random correlations for the Hβ FWHM and the continuum luminosities as well as for the Hβ BLR size and the continuum luminosities.

	r_p	r_s	r_k	P_p	P_s	P_k
NGC 5548: Hβ BLR size vs λL_λ	0.743	0.773	0.600	0.009	0.015	0.010
All AGN: Hβ BLR size vs λL_λ	0.901	0.774	0.613	0	1.556×10^{-7}	1.262×10^{-9}
NGC 5548: FWHM(Hβ) vs λL_λ	-0.029	-0.044	-0.039	0.924	0.871	0.854
All AGN: FWHM(Hβ) vs λL_λ	-0.257	-0.342	-0.241	0.081	0.020	0.017

- strong correlation between Hβ BLR size and luminosity

- (no) correlation between FWHM and luminosity

Kollatschny & Zetzl, 2013c

Comparison of BLR structures in AGN

Scaled with respect to their individual continuum luminosities at 5100Å and with respect to the cont. luminosity of NGC3783.

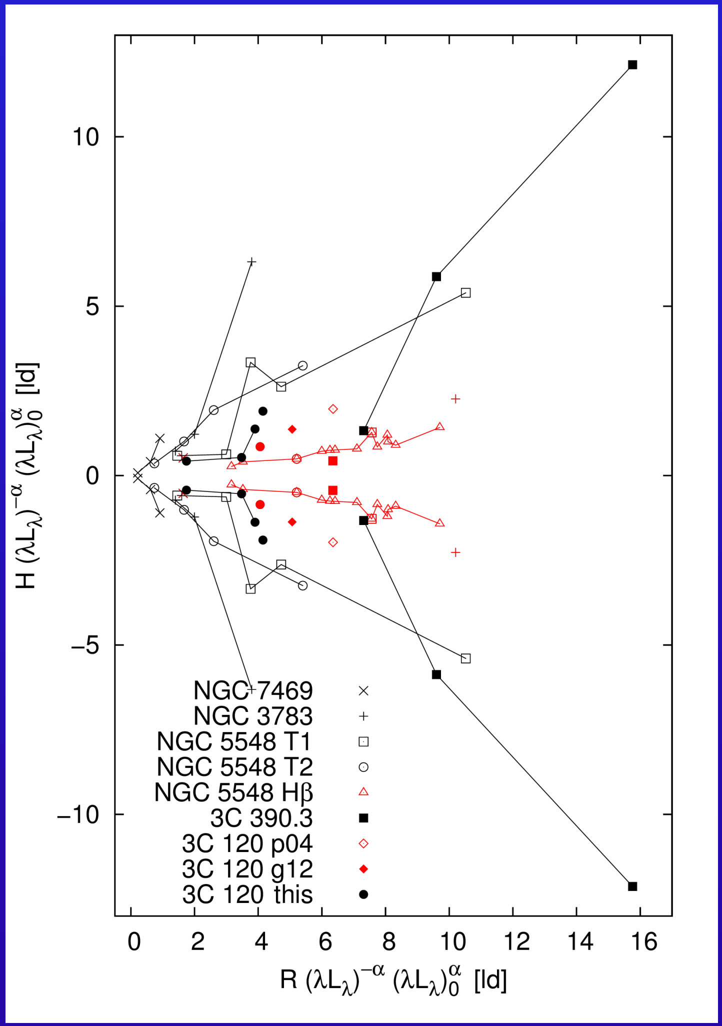

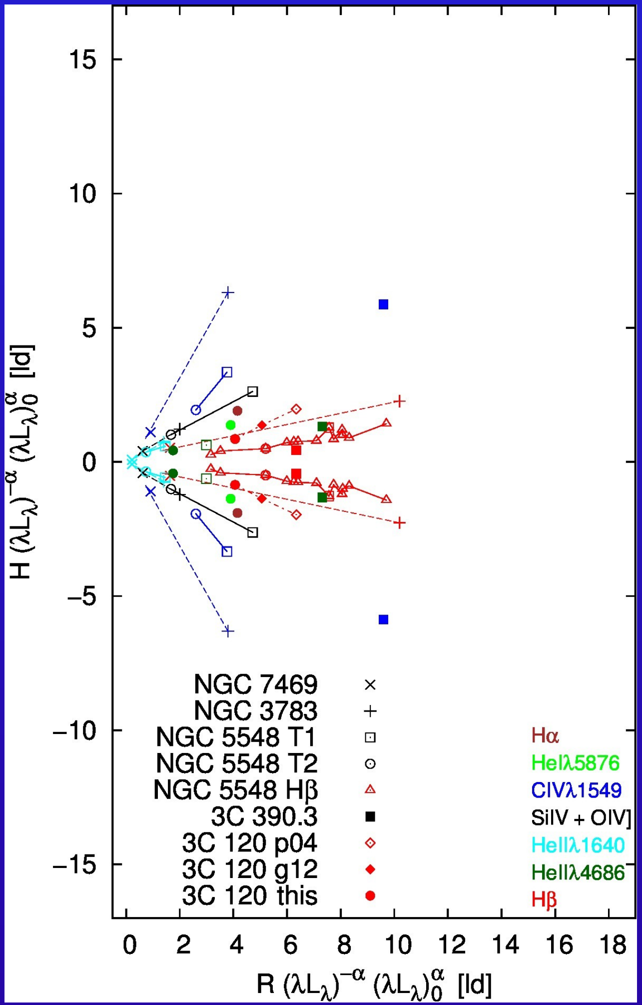

Indiv. galaxies connected by lines. *Indiv. emission lines connected*

Emission lines of galaxies with broader profiles originate closer to the midplane

Comparison of BLR structures in AGN

Scaled with respect to their individual Schwarzschild black hole radii.

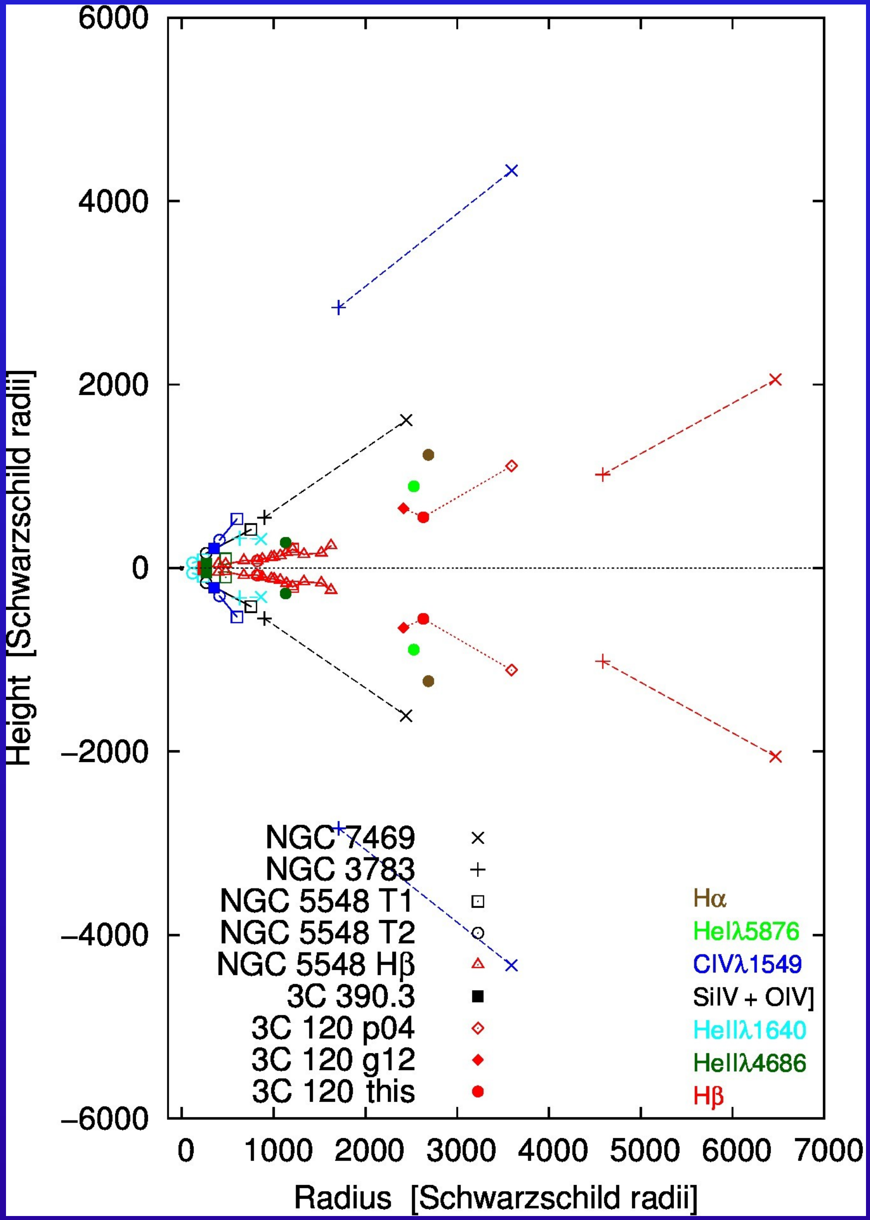

Comparison of BLR structures in AGN

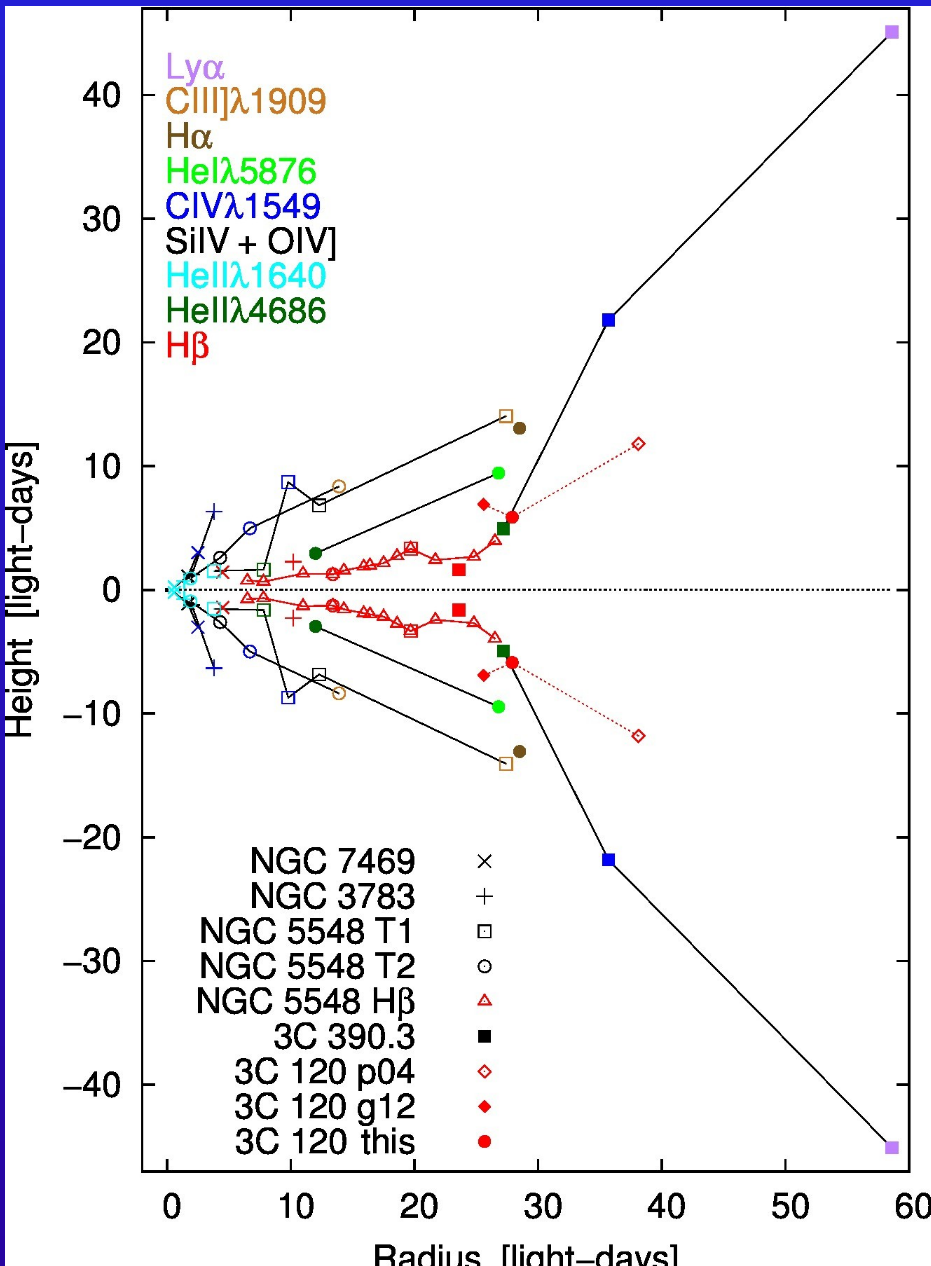

Comparison of the broad line region structures in NGC7469, NGC3783, NGC5548 (two epochs), 3C390.3 and 3C120 as a function of distance to the center as well as height above the midplane.

All the highly ionized emission lines of the individual galaxies are connected by a solid line. Hβ emitting line regions are drawn in red. The Hβ emitting line regions in NGC5548 (13 epochs) are connected by a red solid line.

Emission lines of galaxies with broader profiles originate closer to the midplane.

Kollatschny & Zetzl, 2013c, 2014

Height-to-radius ratio of Hβ emitting regions as fct. of FWHM

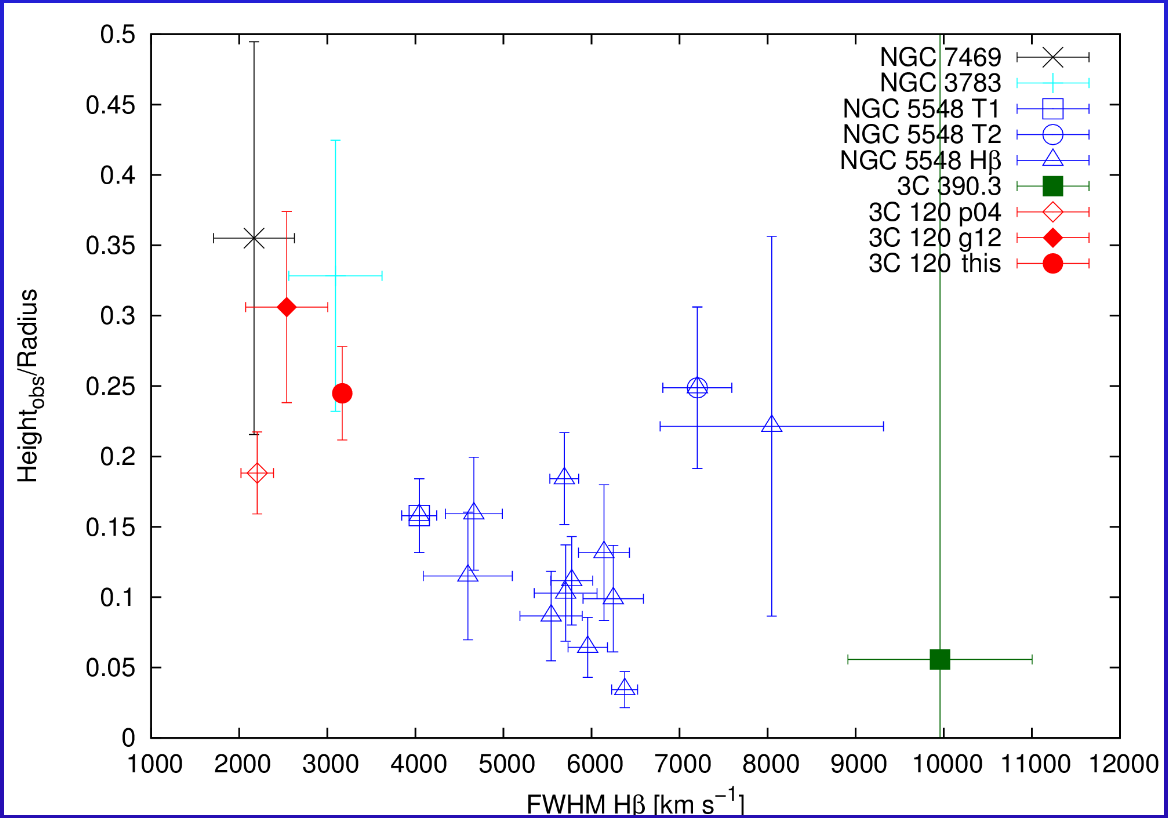

Broader Hβ emission lines originate closer to the midplane than narrower Hβ lines.

This is true for other lines as well.

Kollatschny et al., 2014